PLASTIC FIBER OPTIC HUMIDITY AND GAS SENSOR

by

Sabriye Açıkgöz

BS., in Phys., Marmara University, 2003

Submitted to the Institute for Graduate Studies in
Science and Engineering in partial fulfillment of
the requirements for the degree of
Master of Science

Graduate Program in Physics

Boğaziçi University

2007

ACKNOWLEDGEMENTS

M. S. thesis was very important for me. Because it was the beginning of my academic career. I was lucky because there were many precious people who have helped me for the completion of this work.

In the first place, I would like to thank my thesis supervisor Prof. M. Naci İnci for all the encouragement, foresight and relieving guidance throughout my M. S. thesis study, providing a productive and cooperative atmosphere for research. My particular thanks to Prof. Yani Skarlatos for much help and moral support.

I would like to extend my special thanks to my laboratory colleagues, Özgül, Bükem and Kaan for their support, suggestions and most importantly for their friendship. My special thanks to Özgül for her contributions. She has never failed to give me help during my experimental studies. I have learned from her preparing the samples and using the vacuum system.

I am indebted to all of my family for their spiritual and material support. My mother always loving and full of life has encouraged me for an academic career and has never lost the belief in me in the depressing periods of my thesis. My father have beared with me with his unending patience and kindness.

I finally wish to thank my husband, Erkan, for extending his support in every way and for providing the necessary conditions for the concentrated work that I needed to have. Words cannot suffice to describe how much he supported me during the preparation of this thesis, I could never imaging going through this year without him.

ABSTRACT

PLASTIC FIBER OPTIC HUMIDITY AND GAS SENSOR

In this thesis, a simple and low cost plastic optical fiber (POF) sensor with a humidity sensing range from 13 % to 95 % relative humidity (RH) is described. The sensing mechanism of POF humidity sensor is based on the alterations of refractive index of a polymeric thin film which is coated directly onto a polished segment of plastic optical fiber as cladding layer. When the refractive index of the cladding layer of POF changes, due to the relative humidity, fiber output voltage changes significantly. Gamma-isocyanatopropyltriethoxysilane end-capped polyethylene glycol (PEG-Si), which is a highly hydrophilic polymer, is used as the coated polymer film. At low humidity levels, PEG-Si has a semicrystalline form; therefore, its refractive index slowly decreases with respect to increase in the amount of absorbed water molecules. As a result, the fiber output voltage decreases linearly up to 80 % RH; then, it shows a turning point and fiber output voltage starts to increase. Since PEG-Si melts from the semicrystalline form to a gel form, its refractive index shows a sudden decrease. To overcome this instability problem, PEG-Si polymer layer is enriched with hydrogen. The turning point in the hydrogenated PEG-Si shifts to higher values of relative humidity and the sensor output gives a linear and repeatable response to the humidity. The response of PEG-Si to various gases such as acetone, methanol, hexane, benzene, and toluene is also studied. It is observed that when acetone, methanol, and hexane vapors are increased, the fiber output voltage increased; whereas toluene and benzene decreased the output voltage due to their ring structure and their high refractive index.

ÖZET

PLASTİK FİBER OPTİK NEM VE GAZ SENSÖRÜ

Bu çalışmada % 13 ve % 95 bağıl nem aralığında duyarlı olan basit ve ucuza mal edilebilecek bir plastik fiber optik nem sensörü betimlenmiştir. Bu nem sensörünün duyarlılık mekanizması, kılıf tabakası kazınmış olan fiber üzerine kaplanan polimer filmin kırılma indisinin değişmesi prensibine dayanmaktadır. Bağıl neme bağlı olarak fiberin kırılma indisi değiştiği zaman, fiber çıkış voltajı da önemli ölçüde değişir. Fiber üzerine kaplanacak polimer olarak, yüksek oranda suyu-seven bir polimer olan Gamma-isocyanatopropyltriethoxysilane polyethylene glycol (PEG-Si) kullanılmştır. Düşük nem seviyelerinde, PEG-Si yarıkristal bir yapıya sahiptir ve polimer tarafından emilen su molekülleri miktarı arttıkça PEG-Si'nin kırılma indisi yavaşça azalmaktadır. Sonuç olarak fiber çıkış voltajı da % 80 bağıl nem degerine kadar lineer olarak azalmaktadır. Bağıl nemin % 80'e ulaştığı noktada, fiber çıkış voltajı artmaya başlar ve bir dönüm noktası oluşur. Bunun nedeni % 80 bağıl nem değerinden sonra polimerin yarıkristal yapısının erimesi ve kırılma indisinin aniden azalmasıdır. Bu kararsızlık probleminin üstesinden gelebilmek için, PEG-Si polimeri hidrojen ile zenginleştirilir. Hidrojene edilmiş olan PEG-Si ile kaplanmış olan fiberin çıkış voltajında görülen dönüm noktası daha yüksek bağıl nem değerlerine doğru kaymıştır ve böylece sensör çıkışının bağıl neme duyarlılığı lineer ve tekrarlanabilir bir yapıya sahip olur. PEG-Si kaplanmış olan fiberin aseton, metanol, heksan, toluen ve benzen olmak üzere çeşitli gazlara olan tepkisi de incelenmiştir. Aseton, metanol ve heksan fiber çıkış voltajını arttırırken, toluen ve benzen, halka moleküler yapısına sahip oldukları ve kırılma indisleri yüksek olduğu için, çıkış voltajını azaltmaktadır.

TABLE OF CONTENTS

LIST OF FIGURES

LIST OF TABLES

LIST OF SYMBOLS/ABBREVIATIONS

a	Penetrant activity
Al	Aluminum
b	Core radius
Cl	Chlorine
Co	Cobalt
F	Finesse
H	Hydrogen
I_0	Incident light intensity
K	Potassium
L	Length of fiber
L_T	Loss in transmittance
Mg	Magnesium
N	Nitrogen
n_0	Refractive index of air
n_1	Core refractive index
n_2	Core refractive index
NA	Numerical aperture
O	Oxygen
P_e	Photoelastic constant
P_{in}	The input optical power
P_{out}	The output optical power
R	Mirror reflection
T	Temperature
T_g	Glass transition temperature
V	Mode number
Δ	Normalized index difference
λ	Wavelength
θ_i	Incidence angle

θ_t	Transmission angle
θ_c	Critical angle
α_{max}	Maximum acceptance angle
φ	Volume fraction
χ	Interaction parameter
λ_B	Bragg wavelength
Λ	Grating pitch
ζ	Thermooptic coefficient
ε	Strain
α_{RH}	Moisture expansion coefficient
α_T	Thermal expansion coefficient
ϕ	Round trip phase retardance

FBG	Fiber Bragg grating
FPI	Fabry-Perot interferometer
HEC	Hydroxyethylcellulose
ISAM	Ionic self-assembly monolayer
POF	Plastic optical fiber
PEG	Polyethylene glycol
PEG-Si	Gamma-isocyanatopropyltriethoxysilane end capped polyethylene glycol
PVDF	Polyvinylidenfluoride
PVPA	Poly-vinylpyrrolidone acrylic acid
TIR	Total internal reflection
QCM	Quartz crystal microbalance
PMMA	Polymethylmetcrylate

1. INTRODUCTION

Monitoring and controlling relative humidity and water content are important in many industrial processes such as pharmaceutical manufacturing, food processing and paper production. Standard methods for measuring relative humidity include comparing the temperatures of the wet- and dry-bulb thermometers and observation of chilled mirror dew point depression [1]. However these instruments are bulky and are not amenable to online measurements and monitoring. Most commercially available relative humidity sensors are classified into two general categories, electronical and optical. Electronic relative humidity sensors are based on changes in electronic properties such as current, resistance, capacitance and conductivity [2-7]. On the other hand, optical sensors, which have been developed by using fiber optic cables, are based on absorption [2,8], reflection [9], refractive index [9], anisotropy, luminescence intensity, and luminescence lifetime [10].

Fiber optic relative humidity sensors offer important advantages such as immunity to electromagnetic interference, compatibility with optical fiber data transmission systems, easiness in handling, smallness in size, explosion proof, ability to realize long-distance remote operations, an important feature in noisy industrial conditions, and high sensitivity. Moreover, the fiber optic sensors are intrinsically safe in electrically dangerous environments, whereas electronic sensors are hazardous. For example, a non-electrical device is a distinct advantage in medical applications.

Many techniques have been investigated in order to construct fiber optical relative humidity sensors. Generally, these sensors consist of a polished fiber and an overlay material. The device exhibits a particular attenuation power depending on the refractive index of the external medium in contact with the polished surface. To design a fiber optic sensor, the most important question is which materials should be coated to the fiber as a sensitive cladding layer which can perform a refractive index change as a response to the changes in the environment to be measured. Obviously, for the case of the relative humidity measurements, the aim is to find a suitable material that can

readily absorb and desorb water molecules.

Various metal oxides such as MgO [11], $BaTiO_3$, SnO_2, Al_2O_3 and ZnO [12] have been reported to be used as sensor elements for humidity sensing applications. For example, MgO has coordinately unsaturated sites over its surface and thus it can be utilized as a sensor overlay that absorbs water molecules easily. The effects of the physical adsorption or chemisorption effectively change two parameters of the material, electrical conductivity and refractive index [11]. The charge transfer or proton ion formation gives an increase in electrical conductivity; while the presence of water molecules in the film contributes towards the change in refractive index.

Another approach to look for suitable materials can focus on some inorganic compounds. When inorganic compounds are exposed to water vapor, they can absorb water molecules and form coordination complexes, and change their characteristic colors. For example; the complexes of transition metals, such as Cobalt in $CoCl_2$, alter their coordination number and the originally anhydride blue form changes to pink due to water absorption. For the purpose of detecting humidity, the change in the spectral absorption of $CoCl_2$ which is entrapped in a polymer [13] or gelatin [14,15] host is studied. The fiber evanescent wave can interact with this overlay sensing film and water molecules can penetrate into the film and interact with the $CoCl_2$ to change its absorbing properties. Furthermore, overlay material and cobalt chloride changes its refractive index depending on the relative humidity of its environment and this change induces variations in the transmitted power along a polished fiber. Because of these properties, $CoCl_2$ can be used as a proper material in order to construct a relative humidity sensor. However, these sensors have some disadvantages such as requiring multimode fibre and the use of visible wavelengths that make them unsuitable for using in the telecommunications network [16].

Certain kinds of polymers and cellulose such as hydroxyethylcellulose (HEC) [17,18] can also be used as a proper material to measure the relative humidity value of an environment. Poly-vinylpyrrolidone acrylic acid (PVPA), Polyvinylidenfluoride (PVDF) [19] and Polyethylene glycol (PEG) [5,16,20] are some polymers which are

sensitive to high water vapor. They undergo swelling due to attachment of water molecules and show a decrease in refractive index. In order to fabricate a humidity sensor head, these polymers and cellulose are coated on the fiber core substrate as a functional cladding layer. When this sensor head is exposed to water vapor, the refractive index in the cladding layer begins to decrease and the light intensity passing through the sensor head changes remarkably. The relative humidity level can be predicted with respect to changes in the light intensity.

In this work, our aim is to fabricate a humidity sensor by using a plastic optical fiber (POF). This humidity sensor is based on side-polished optical fiber covered by a polyethylene glycol polymeric film. Polyethylene oxide or Polyethylene glycol (PEG) is known to be highly hydrophilic in its response to water vapor. This makes PEG the most suitable overlay material to detect the relative humidity. However, PEG has a stability problem, it dissolves easily at high humidity when exposed to water vapor; therefore, it is not durable on the substrate. To covalently link this polymer layer to the plastic fibre surface, gamma-isocyanatopropyltriethoxysilane is used in this study [21]. Triethoxysilane allows us to cross-link the PEG network itself as well as the overlay on a polished polymethylmetcrylate (PMMA) plastic optical fibre surface so that it becomes a durable and robust sensing material.

In this thesis, the change in the sensor output voltage which depends on the light intensity passing through triethoxysilane capped polyethylene glycol (PEG-Si) coated plastic optical fibre is experimentally determined as a function of relative humidity. Besides relative humidity, the response of PEG-Si to some gases such as acetone, methanol, toluene, hexane and benzene and the effects of these gases on the sensor output voltage are studied.

This study consists of four chapters. This first chapter provides an introduction to why our fiber optic sensor is preferred over conventional sensors and summarizes some advantages of this type of sensors; and which overlay materials would be suitable for relative humidity sensing applications.

The second chapter of the thesis is devoted to a brief review of the plastic optical fiber (POF) and water absorption mechanism of the polyethylene glycol. In addition, this chapter gives some basic information about previous fiber optical humidity sensors.

In the third chapter of this thesis, the change in the output voltage, which is related to the light intensity passing through the polymer coated fiber, is experimentally measured for the relative humidity ranging from 13 % to 95 %. When PEG is dry, its refractive index is 1.46 [22], which is very close to the core refractive index (1.49). Hence, coupling occurs and a fraction of the power in the fiber core is lost into the overlay. As a result, the sensor head operates as a leaky-type POF. When PEG-Si is exposed to water vapor, the fiber output voltage decreases as relative humidity increases up to 80 %. PEG-Si polymer film has a semicrystalline form at low humidity values; therefore, its refractive index slowly decreases with respect to increase in the amount of the absorbed water molecules [22]. Beyond 80 % relative humidity value, it is observed that there is a turning point as a result of the instability problem of the polymer. At that point, the polymer film changes phase from a semicrystalline form to a gel form because of that PEG-Si melts at high humidity levels. After swelling, the refractive index of polymer shows a sudden decrease and it becomes 1.41 at around 80 % [22]. Then, the POF structure changes to the guided-type and fiber output voltage starts to increase. To alleviate the stability problem of the PEG-Si film at high rh values, and to increase the range of the sensor , PEG-Si is enriched with hydrogen. Thus, the turning point shifts to higher humidity values and the sensor output gives a linear, reversible, fast and repeatable response to humidity. In the last part of this chapter, we studied with various gases to determine the effects of these gases on the fiber output voltage. Benzene and toluene has a ring structure; therefore, the response of PEG-Si to methanol and acetone is higher than that of the benzene and toluene.

The last chapter focuses on the brief history of this work, followed with the future promises and recommendations.

2. REVIEW

2.1. General Outline

Fiber optic sensors can be classified into three categories according to the means of sensing, the extent of sensing and the role of optical fibers. In terms of the means of sensing, sensors are grouped as intensity sensors or interferometric sensors according to whether they are based on intensity or phase changes. Intensity sensors include devices based on scattering, attenuation and change in the mode of propagation inside the fiber. Interferometric sensors are based on monitoring phase induced changes arising from changes in the optical path length. The classification is based on the extent of sensing group devices as distributed and point sensors. While distributed sensors detect changes of the physical quantities continuously along the fiber length, point sensors are sensitive over a limited distance. Finally, sensors are classified as intrinsic or extrinsic sensors depending on whether the device is fiber itself or the fiber merely serves to transport the signal. With extrinsic sensors, light leaves the fiber and is blocked or reflected before going back into the fiber-optic system. Extrinsic sensors are, in general, analogous to photoelectric controls with the potential problems of being affected by dirt, dust, vibration, and alignment. Intrinsic sensors avoid these problems by changing the light while it is still inside the fiber.

2.2. Optical Fibers

An optical fiber is a cylindrical dielectric waveguide which is designed to guide light along its length by total internal reflection and is made of low loss materials; such as silica glass or special polymers (PMMA) [23]. Optical fibers are widely used in fiber-optic communication, which permits digital data transmission over longer distances and at higher data rates than electronic communication. They are also used to form sensors, and in a variety of other applications.

The most widely accepted waveguide structure is a single solid cylinder known

as the core of the fiber in which light is guided. The core is surrounded by a solid dielectric cladding having a refractive index less than that of the core [24]. There are two types of fibers, step-index and graded-index fiber. In the step-index fiber, the refractive index of the core is uniform and undergoes an abrupt change at the cladding boundary. In the graded index fiber, the core refractive index is not constant within the core but decreases from n_1 at the center, as a function of radial distance from the center of the fiber, to n_2 at cladding boundary (see Figure 2.1).

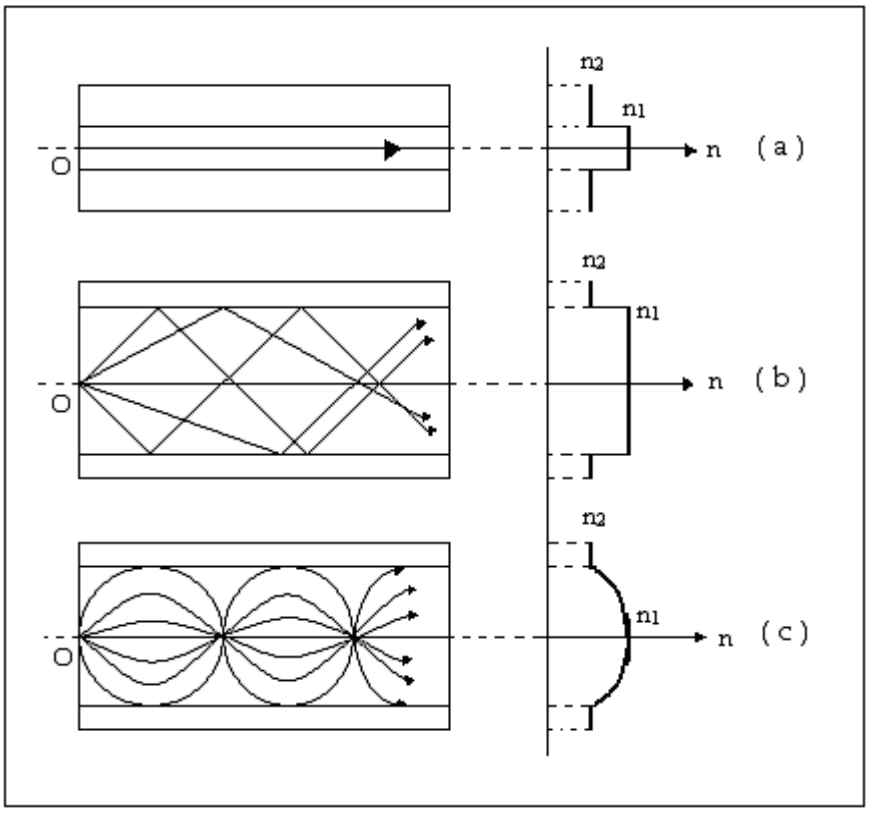

Figure 2.1. (a)Monomode step-index fiber, (b) Multimode step-index fiber, (c)Multimode graded-index fiber

Optical fibers are also classified as single-mode and multimode fibers with respect to their number of modes. Single mode fibers are designed by choice of core radius and normalized index difference ($\triangle = (n_1 - n_2)/n_2$) , to allow only the fundamental mode to propagate at the required wavelengths [25]. Typically, single mode fibers have a very small core radius. It is used where the modulation requires the maintenance of spatial coherence as in the case of time or phase [26]. Thus, it should be excited with

laser diodes. The number of the modes in a fiber depends on the V - number which is given by

$$V = \frac{2\pi b}{\lambda}(n_1^2 - n_2^2)^{\frac{1}{2}}. \tag{2.1}$$

If the V - number is smaller than 2.405; then, a single mode fiber is obtained. Otherwise, the fiber is defined as a multimode fiber. In multimode fibers, light propagates through many modes and these are mainly all confined to the core. This type of fibers are generally used for intensity and wavelength modulations. One of the advantage of multimode fibers is the possibility of launching light into the fiber by the use of light emitting diode (LED) [27].

Light propagation in optical fibers is based on the total internal reflection in an optical waveguide as explained below.

2.2.1. Total Internal Reflection

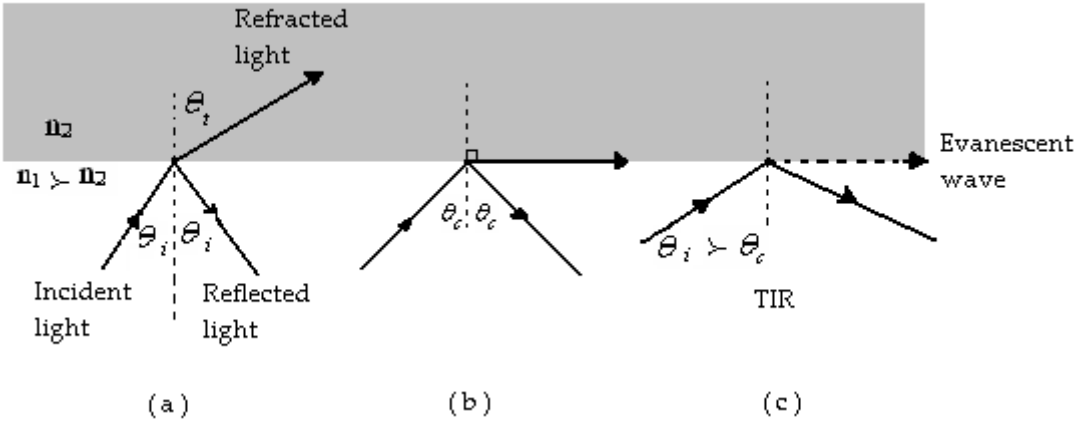

Figure 2.2. Representation of the critical angle and total internal reflection

Total internal reflection can occur when light is directed from a medium having a given index of refraction toward one having a lower index of refraction. When a ray is incident on the interface between two dielectrics of differing refractive indices, refraction occurs as shown in Figure 2.2. It is observed that the incident ray is propagating in a dielectric of refractive index n_1 and incidence angle θ_1. When a ray of light travelling

through a transparent medium encounters a boundary leading into another transparent medium that has a refractive index n_2 ($n_2 < n_1$), part of the ray is reflected back into the first medium and the remainder is refracted. It enters the second material with an angle θ_2 which is greater than θ_1. The angle of refraction, θ_2, depends on the optical properties of the two media and the angle of incidence through the relationship that is known as *Snell's law* and given by

$$n_1 \sin\theta_1 = n_2 \sin\theta_2. \tag{2.2}$$

The refracted ray is bent away from the normal because n_1 is greater than n_2. At some particular angle of incidence θ_c, called the critical angle, the refracted light ray moves parallel to the boundary so that $\theta_2 = 90^0$. The critical angle is given by

$$\sin\theta_c = \frac{n_2}{n_1}. \tag{2.3}$$

When the incidence angle θ_i exceeds θ_c then there is no transmitted wave but only a reflected wave. The latter phenomenon is called total internal reflection. The effect of increasing the incidence angle is shown in Figure 2.2.

2.2.2. Numerical Aperture and Acceptance Angle

Not all source radiation can be guided along an optical fiber. Only rays falling within a certain cone at the input of the fiber can normally be propagated through the fiber. Figure 2.3 shows the path of a light ray launched from the outside medium of refractive index n_0 into the fiber core. Consider a ray with an angle α enters the core and inside the waveguide the ray makes an angle θ with the normal to the fiber axis. Unless the angle θ is greater than the critical angle θ_c, the ray will escape into the cladding. It is obvious that α takes its maximum value for $\theta = \theta_c$ and this maximum

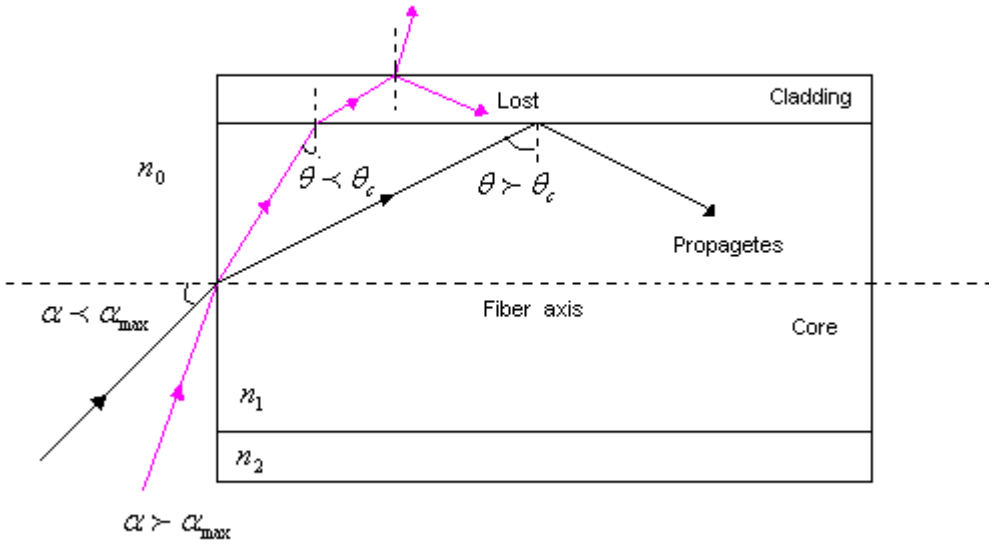

Figure 2.3. Maximum acceptance angle α_{max}

angle is called *acceptance angle*. At the $\frac{n_0}{n_1}$ interface, Snell's law gives

$$n_0 \sin \alpha_{max} = n_1 \sin(90^0 - \theta_c) \tag{2.4}$$

$$\sin \alpha_{max} = \frac{n_1}{n_0} \cos \theta_c \tag{2.5}$$

$$\sin \alpha_{max} = \frac{n_1}{n_0}(1 - \sin^2 \theta_c)^{\frac{1}{2}}. \tag{2.6}$$

in which $\sin \theta_c$ is determined by the onset of total internal reflection, that is $\sin \theta_c = \frac{n_2}{n_1}$. We can now eliminate θ_c to obtain,

$$\sin \alpha_{max} = \frac{\sqrt{n_1^2 - n_2^2}}{n_0}. \tag{2.7}$$

The *numerical aperture* NA is a characteristic parameter of an optical fiber de-

fined by

$$NA = \sqrt{n_1^2 - n_2^2} \tag{2.8}$$

so that in terms of NA , the *maximum acceptance angle*, α_{max}, becomes

$$\sin \alpha_{max} = \frac{NA}{n_0}. \tag{2.9}$$

2.2.3. Attenuation In Optical Fibers

An optical signal is degraded by attenuation and dispersion as it propagates through a material. While dispersion can sometimes be eliminated, attenuation simply leads to a loss of signal [28]. Attenuation emerges from several different physical effects such as intrinsic material absorptions, absorptions due to impurities, Rayleigh scattering and micro bending loss. Intrinsic material absorption is the most serious cause of power loss. Suppose that the input optical power into a fiber of length L is P_{in} and the output optical power at the end of the fiber is P_{out} and intensity anywhere in the fiber at a distance x from the input is P. The *attenuation coefficient* α is defined as [28]

$$\alpha = -\frac{1}{P}\frac{dP}{dx}. \tag{2.10}$$

If it is integrated over the length L of the fiber, it is found that

$$\alpha = \frac{1}{L}\ln(\frac{P_{in}}{P_{out}}). \tag{2.11}$$

If α is given, then P_{out} can be calculated from P_{in} through,

$$P_{out} = P_{in}\exp(-\alpha L). \tag{2.12}$$

2.3. Fiber Optic Relative Humidity Sensors

2.3.1. Fiber Bragg Grating Relative Humidity Sensors

Fiber Bragg gratings (FBGs) are used extensively in the telecommunication industry. A FBG behaves like a spectral filter which has inherent characteristics that render it very sensitive to strain and temperature. Applications of FBGs are also gaining widespread popularity in the humidity sensing sensors.

A FBG is formed by photoinduced refractive index modulation in the core of a single mode fiber. The structure formed within the fiber behaves like a notch filter which reflects the light signal at a wavelengths termed Bragg wavelengths (λ_B) that satisfy the Bragg conditions. The value of the Bragg wavelengths is determined by [29]

$$\lambda_B = 2n_{eff}\Lambda \tag{2.13}$$

where n_{eff} is the effective refractive index of the optical fiber and Λ is the grating pitch. These FBGs are very popular in strain and temperature sensing applications. The shift in the Bragg wavelength due to the change in strain or thermal effect is given by

$$\frac{\Delta\lambda_B}{\lambda_B} = (1 - P_e)\varepsilon + [(1 - P_e)\alpha + \zeta]\Delta T \tag{2.14}$$

where P_e is the photoelastic constant of the fiber, ε is the strain induced on the fiber, α is the fiber thermal expansion coefficients and ζ is the thermooptic coefficient. To apply the above equation in a humidity sensing, a slight modification is required to the above strain effect induced FBG by the swelling of the humidity sensitive polymer. The shift in the Bragg wavelength for the polymer coated FBG is given by

$$\frac{\Delta\lambda_B}{\lambda_B} = (1 - P_e)\alpha_{RH} \cdot \Delta RH + [(1 - P_e)\alpha_T + \zeta]\Delta T \tag{2.15}$$

where α_{RH} and α_T are the moisture expansion coefficient and the thermal expansion

coefficient of the coated FBG. The above equation can be further simplified to

$$\frac{\Delta\lambda_B}{\lambda_B} = (1 - P_e)\varepsilon_{RH} + (1 - P_e)\varepsilon_T + \zeta\Delta T. \tag{2.16}$$

The shift in the Bragg wavelength depends on three components, the strain effect induced on the FBG due to moisture, the thermal expansion and the thermooptic effect.

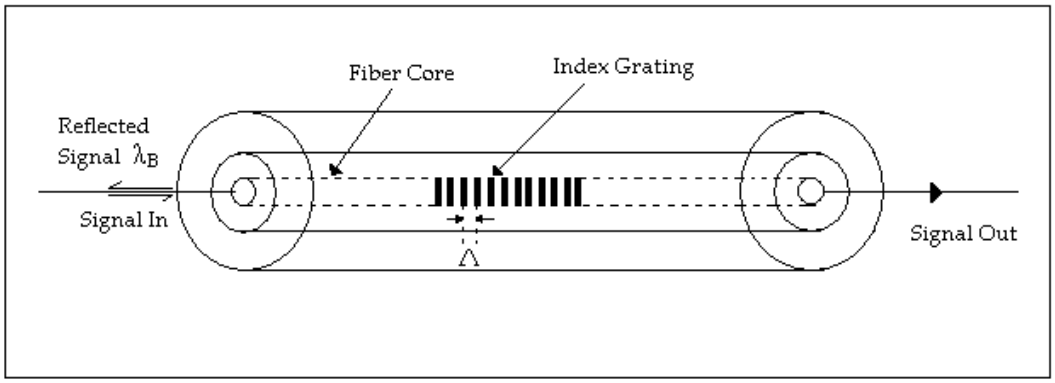

Figure 2.4. Fiber bragg grating

Gratings are written into a single mode fiber by using a phase mask and an eximer laser. FBG samples are dip-coated with a polymer solution to form the sensing element (see Figure 2.4). The Bragg wavelength shift is observed for different humidity values. As the humidity increases, the wavelength is found to shift toward the longer wavelength which is consistent with the elongation of the FBG caused by the expansion of the polymer coating [30].

The polymer coated FBG is modeled as a composite bar consisting of two materials which are tightly bounded together. When the bar is exposed to humidity change, the resultant of the extension and compression force developed on the two materials, each with different expansion coefficients causes the bar two expand. The strain acting on the FBG due to the moisture expansion of the polymer coating can be given by [30]

$$\varepsilon_{RH} = [\frac{A_p E_P}{A_p E_p + A_f E_f}] \cdot (\alpha_{pRH} - \alpha_{fRH}) \cdot \Delta RH \tag{2.17}$$

where A_p and A_f are the cross sectional areas of the polymer and fiber (p=polymer, f=fiber), E_p and E_f are the Young's modulus of the materials and α_{pRH} and α_{fRH} are the moisture expansion coefficients of the materials. By using this theory, the moisture expansion of the polymer can be calculated.

2.3.2. Fabry-Perot Interferometer Relative Humidity Sensors

The Fabry-Perot interferometer (FPI), sometimes called the Fabry-Perot etalon, consists of two mirrors of reflectance R_1 and R_2 separated by a distance L. Fiber Fabry-Perot interferometers are used in the sensing of temperature, strain, pressure and humidity. The sensing region consists of the portion of the fiber core (or in some cases an air gap) between the two mirrors. The Fabry-Perot interferometer can be used in either transmission or reflection mode and it is described by the transfer function

$$I = \frac{I_0}{1 + F\sin^2(\phi/2)} \tag{2.18}$$

where I_0 is the light intensity incident on the cavity, ϕ is the round trip phase retardance which is given by

$$\phi = \frac{4\pi nl}{\lambda} \tag{2.19}$$

where n is the effective refractive index of the fiber core and l is the physical length of the fiber cavity, F is the phase resolution of the device,

$$F = \frac{4R}{(1-R)^2} \tag{2.20}$$

where R is the mirror reflection. The transfer function of the Fabry-Perot is a periodic series of sharp transmission peaks where the maximum of each peak is centered on $\phi = 0$ modulo π [31].

In order to make humidity sensitive Fabry-Perot interferometer, anionic polymers can be used [32]. By using ionic self-assembly monolayer (ISAM) technique, a bilayer

structure is built up at the end face of an optical fiber. The parallel layer structure of the coating forms an interferometric cavity and this structure behaves as a nano Fabry-Perot cavity, as shown in Figure 2.5.

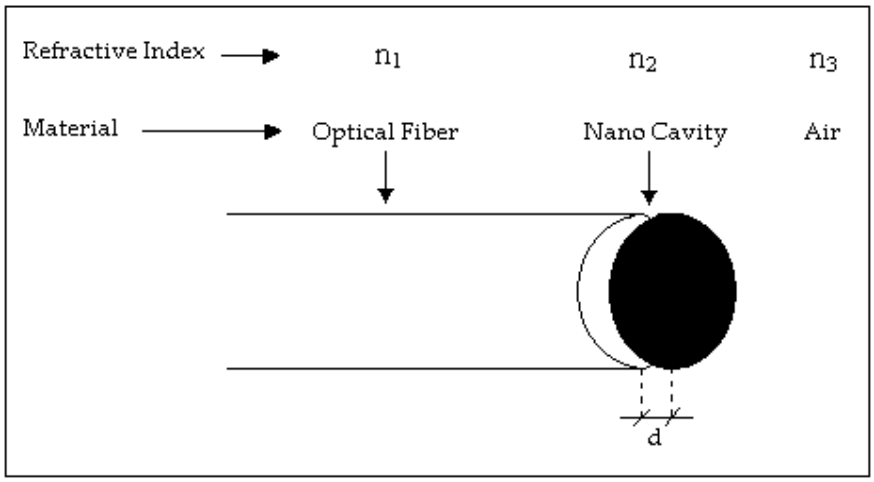

Figure 2.5. Fabry-Perot interferometer relative humidity sensor

In this interferometric cavity, the mirrors are formed by the refractive index differences between the different optical media at either end. The reflectance of each mirror is determined by Fresnel's law,

$$R_1 = \frac{(n_1 - n_2)^2}{(n_1 + n_2)^2} \tag{2.21}$$

$$R_2 = \frac{(n_2 - n_3)^2}{(n_2 + n_3)^2} \tag{2.22}$$

where R_1 is the reflection coefficient of the first interface (optical fiber/coating) and R_2 is the reflection coefficient of the second interface (coating/air). The change in the intensity of reflected (or transmitted) optical power depends on the reflection of the external mirror at the end face of the optical fiber, R_2. Changes in the R_2 with humidity can be achieved because the coating material is hygroscopic.

2.3.3. Air Gap Design Relative Humidity Sensors

A novel optical configuration for humidity sensors is characterized by an air gap design. Two optical fibers are fixed face to face with each other so that a small air gap existed between the two fibers. One or both end faces of the fibers are coated with a humidity sensing film as shown in Figure 2.6. This configuration reduces the size of the sensors and also reduces the loss of the light transmitted through the sensing region.

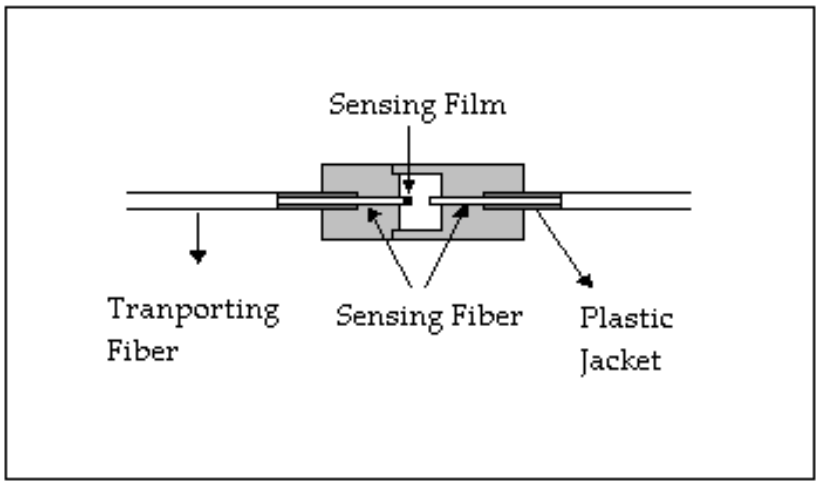

Figure 2.6. Schematic diagram of an air gap design humidity sensor

An air gap between two optical fibers often occurs when the fibers are incorrectly connected. The existence of an air gap between fibers will produce loss in transmission of the light. The loss in transmittance L_T for step index multimode fibers is [33]

$$L_T = \frac{S}{2a} \tan \theta_c \tag{2.23}$$

under the condition that

$$S < \frac{a}{2 \tan \theta_c} \tag{2.24}$$

where

$$\theta_c = \sin^{-1} \frac{NA}{n}. \tag{2.25}$$

S is the distance between the ends of two fibers, a is the diameter of the core, θ_c is the critical angle for the fiber, NA is the numerical aperture, and n is the refractive index of the air. The intensity of the light transmitted is strongly affected by the relative humidity. The relative humidity value of an environment can be predicted according to the changes in the light intensity.

2.3.4. Side-Polished Fiber Optic Relative Humidity Sensors

Side polishing is a conventional method to construct a relative humidity sensor. When the optical fiber is laterally polished, access is gained to the evanescent field of the guided wave. Fiber optic devices consisting of a polished fiber and an overlay material exhibit a particular attenuation pattern depending on the refractive index of the external medium in contact with the polished surface. Most polymers can easily absorb water and the physical properties of the polymers changes significantly. The main effect of absorbed water on polymeric matrices is plasticization, that is lowering of the glass transition temperature (T_g), thereby dramatically reducing the modulus of the polymer at elevated temperatures [29]. In addition, sorption of water molecules causes swelling of the polymers and their refractive index decreases suddenly.

Hygroscopic polymers, generally, are dip-coated onto the polished optical fiber as a cladding layer (see Figure 2.7). When a polymer is dry, the refractive index of the cladding layer is larger than that of the fiber core and the plastic fiber operates as a leaky-type POF. After the polymer absorbs water molecules, the refractive index in the cladding layer begins to decrease and becomes lower than that of the core. Then the POF structure changes to the guided-type, and light intensity passing through the sensor head increases remarkably. The net result can be predicted as an attenuation gap for values below and above the effective refractive index of the fiber, having a minimum in transmitted optical power when the external medium equals that of the

fiber. With respect to changes in the light intensity, a relative humidity sensor that shows good sensitivity over the wide humidity range can be fabricated.

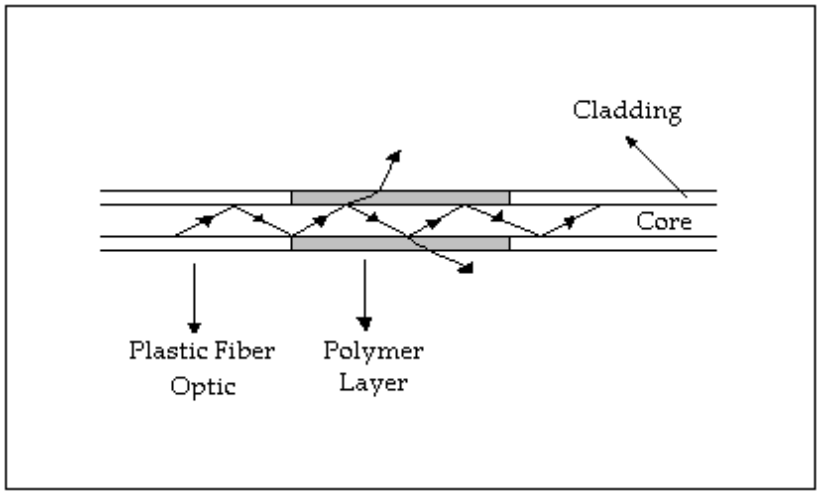

Figure 2.7. Polymer coated fiber optic humidity senor

2.4. The Water Sorption Mechanism In Polymers

Polymer films and their sorption mechanism are currently being investigated due to their theoretical and practical significance. The hydrophilicity of the constituent groups of the polymer is the one of the most important factors affecting water sorption properties. The water sorption of the polymer depends on the intermolecular forces between those groups and water molecules such as electrostatic, directional, inductive forces and hydrogen-bonding forces [34]. The water sorption changes chemical and physical properties of the polymers because the polymer becomes swollen [35]. In determining these swelling-induced changes, various techniques have been used such as the quartz crystal microbalance (QCM) analysis [36], X-ray [37], neutron reflectivity [38], ellipsometry [38] and the solvatochromic method [34].

Polyethylene glycol is a highly hydrophilic polymer, which can easily absorb and desorb water molecules. Besides water molecules, PEG is also a “protein friendly” surface; therefore, it can be used for construction of endovascular medical devices [39].

Before absorbing water molecules, PEG has a semicrystalline form. Due to the strong tendency to absorb water, the melting transition of the crystallites can be induced by contact with sufficiently humid air; then, polymer swells and changes its phase from semicrystalline form to a gel form [40].

According to *the localized sorption theory*, the penetrant is considered to bind at specific sites in the polymeric structure, e.g. in cracks, pores, or at specific polar groups which are capable of interaction with polar penetrants like water. Another approach for penetrant sorption is *dissolution theory*. The starting point of this theory is that for polymer-penetrant systems that do not display strong interactions, observed deviations from ideal behavior should be attributed to the incompatibility of their molecule sizes. This basic concept is known *the Flory-Huggins* relation and it is given by [41,42]

$$\ln(a) = 1 - \varphi + \ln(\varphi) + \chi(1-\varphi)^2. \tag{2.26}$$

In this model, φ is the volume fraction of dissolved penetrant, and a is the penetrant activity. The compatibility of polymer and penetrant is expressed by a dimensionless interaction parameter χ. According to Flory the theory is limited to relatively apolar systems, interacting only weakly. In contrast to that starting point, the Flory-Huggins relation is also used for fitting water sorption.

In the PEG films, the van der Walls force and the ether oxygen are effected by the amount of the water absorbed. The influence of the van der Walls force on the sorption process is very weak. The water molecules in the PEG film dominantly sorb to ether oxygen atom in the PEG chains. This is because the binding energy of the van der Walls interaction is much smaller than that of the hydrogen bonding [43].

The water molecules can bind to the ether oxygen in three different ways [43] (see Figure 2.8).

i) Hydrogen atom of water molecules can form a monomeric bonding to the ether oxygen atom of the polymer (*binding water*).

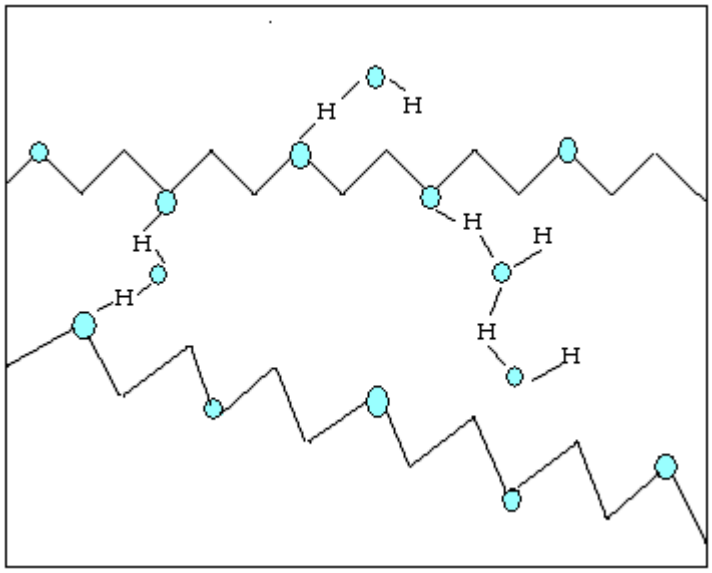

Figure 2.8. The illustration of the binding of water molecules to PEG molecules [43]

ii) A water molecule can bind to another water molecule which is already bound to PEG with hydrogen bonding (*water molecules are dimeric*).

iii) A water molecule can form hydrogen bonds to two PEG chains (*bridging water*). It is also possible that a water molecule hydrogen bonds to neighboring ether oxygen atoms in the same PEG chain (which is also categorized in *bridging water*).

According to the measurements of Kitano et al., the amount of sorbed water indicates that water molecules bind to the PEG mostly monomolecularly and that the amount of monomeric water in the PEG film is much larger than that of the binding water [43]. The process of sorption of water followed by the penetration into the polymer matrix is clarified as follows: At the polymer surface, monomeric water binds to the oxygen atom of the polymer, and the bridging water is formed. The formation of dimer is completed after the water sorption in the polymer matrix is equilibrated. In the polymer matrix, the bridging water is equilibrated first, and subsequently the binding water is equilibrated. Finally, the dimeric water is equilibrated by the attachment of a water molecule to the binding water.

3. EXPERIMENTAL WORK AND RESULTS

3.1. Synthesis of Gamma-isocyanatopropyltriethoxysilane Capped Polyethylene Glycol (PEG-Si)

Our PEG-Si Samples and POF sensor head are prepared using the procedure given in Ref [21,44,45]. 3.75 millimoles of hydroxyl ended PEG ($4000 g/mol$) are dissolved in 180 ml reagent grade toluene. The PEG solution is refluxed in a Dean- Stark apparatus for 3 hours to remove humidity trapped in PEG. The dried PEG / toluene solution is treated with 7.5 millimoles of gamma-isocyanatopropyltriethoxysilane at 323 K overnight. The product is kept at 250 ml equivolume ethanol and methanol mixture for 24 hours at 253 K. The precipitate is filtered with a Buchner funnel at 273 K and is dried at room temperature by using filter paper.

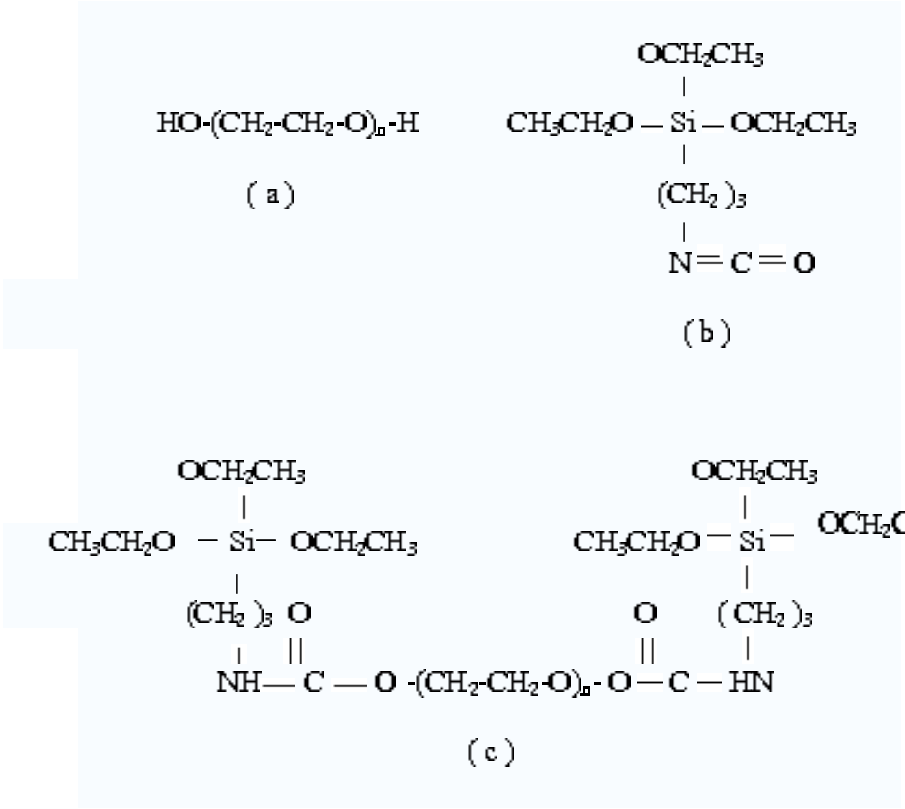

Figure 3.1. (a)PEG,(b)Gamma-isocyanatopropyltriethoxysilane, (c)PEG-Si

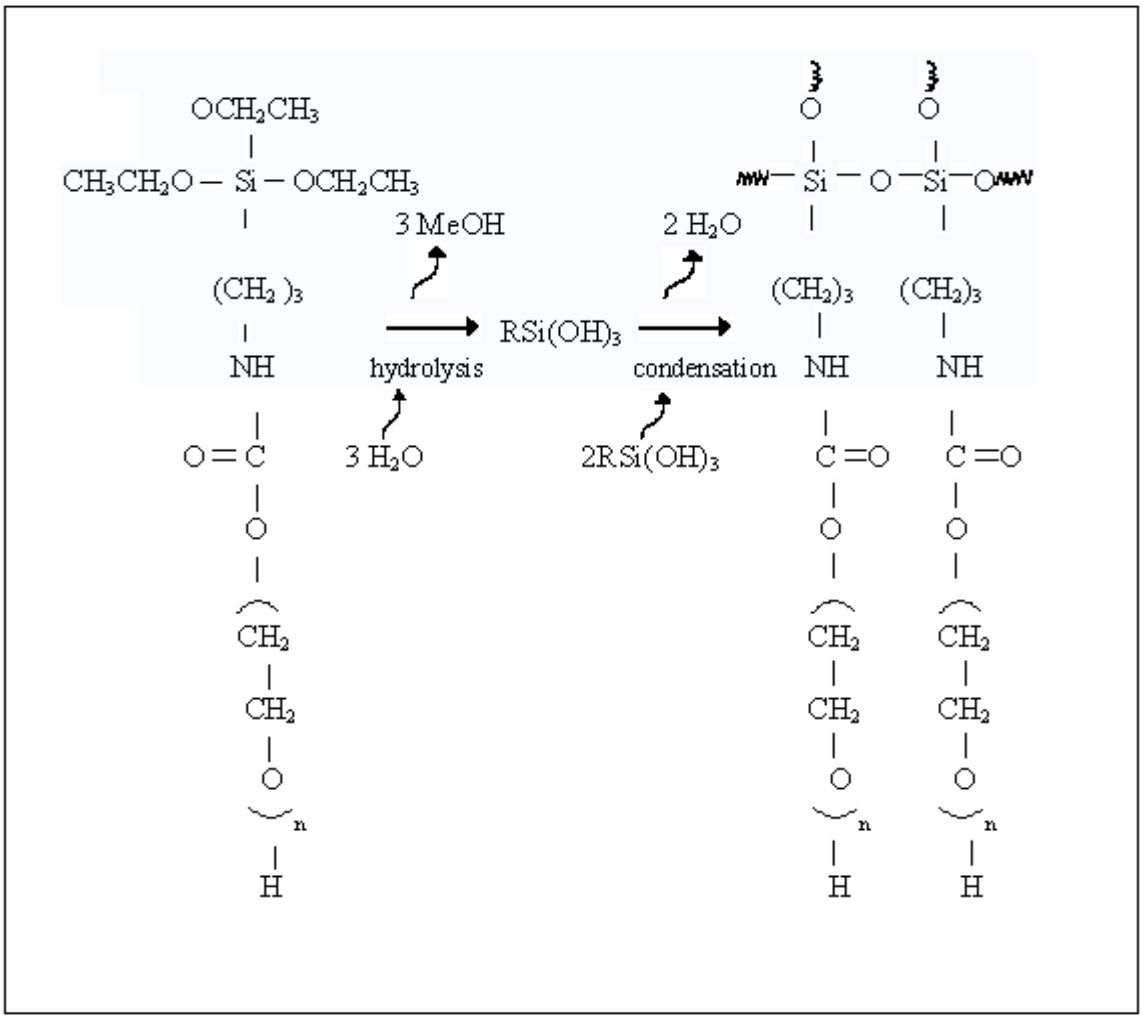

Figure 3.2. Film formation on PMMA substrate

3.2. Preparation of POF-type Sensor Head

2.5 g end group modified PEG, that is, PEG-Si reaction as described above, is dissolved in 500 ml double distilled water. Plastic optical fiber (POF) is used as a sensor substrate. Before coating the POF, both ends of it are polished by using three different sandpapers. Then a 2 cm segment of the cladding layer is removed with a knife from the center of the POF (see Figure 3.3). Dip-coating is used to coat the fiber. A POF fiber is submerged into the polymer solution. POF remains stationary and the solution is made to flow with a constant speed. The constant and very slow flowing speed helps to obtain a thin polymer film which has a uniform thickness. Finally, PEG-Si coated fiber is dried in oven at 323 K for two hours to cross link the film on the

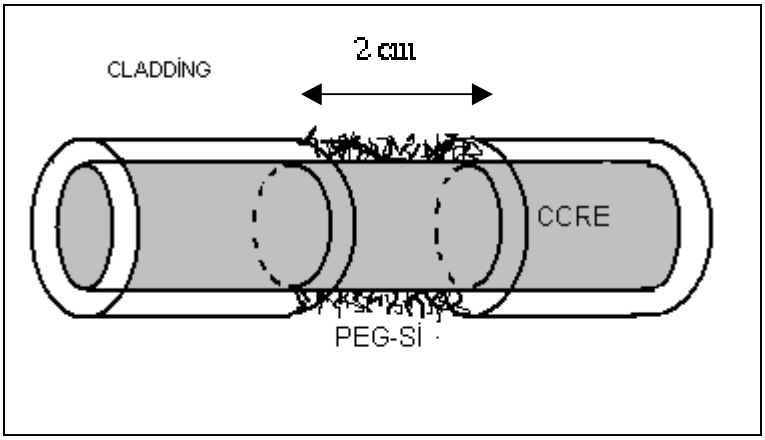

Figure 3.3. PEG-Si film on PMMA substrate

polished segment of the plastic optical fiber.This cross-linked structure is depicted in Figure 3.2 [21]. In order to determine the effects of the film thickness on the hysteresis of the POF sensor, two different samples are prepared. Sample 1 is coated by allowing the polymer solution to flow with a constant speed of 10 ml/min. By this method, a thin sample is acquired. To increase the film thickness, this is Sample 2, three coatings are done on the sensor head.

3.3. Optical Setup

The experimental setup for the characterization of the humidity sensor is shown in Figure 3.4. To reduce the cost of the sensor and prevent unwanted coherent reflections, instead of a laser diode, an infrared light-emitting diode (LED) is used as an illuminating monochromatic incoherent source to monitor humidity measurements. It has a peak wavelength 960 nm, a viewing angle of 20^0 and the maximum voltage $1.8V$.

In the experiment, the POF type fiber (Mitsubishi Rayon Co., $Ck-60$) is used as a sensor substrate because of its low cost and flexibility. The special properties of this type fiber is given in Table 3.1. The total length of the fiber is about 40 cm.

The coated samples are fixed inside a humidity chamber. During the experiments two different humidity chambers are used in order to alter ramp rate of the humidity. One of them has a small volume of $5,5\times4,5\times6$ cm^3 , the other has a volume of $12\times8\times8$

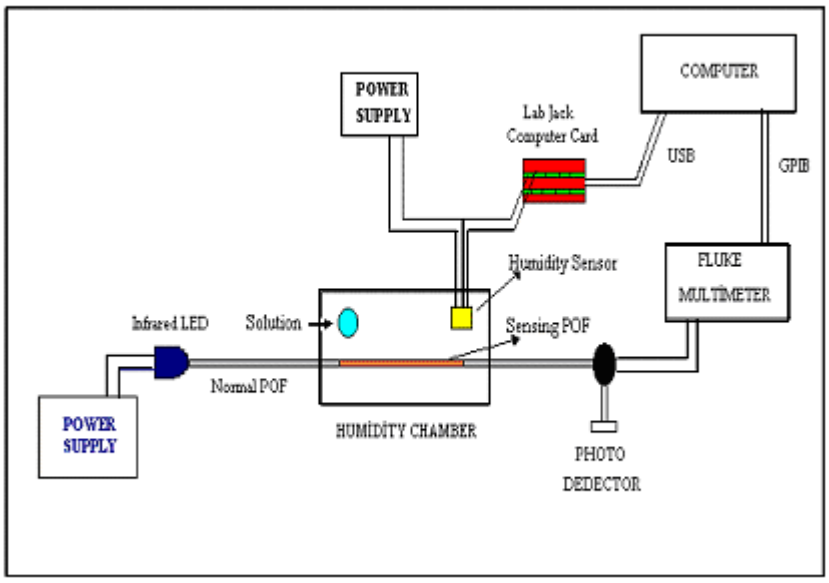

Figure 3.4. Setup used in the measurements

Table 3.1. Properties of plastic optical fiber used

Core Material	Polymetyl-Methacrylate
Cladding Material	Fluorinated Polymer
Core Refractive Index	1.49
Numerical Aperture	0.5
Refractive Index Profile	Step Index
Core Diameter	1.470 μm
Cladding Diameter	1.500 μm
Approximate Weight	2,2 g/m

cm^3. For the purpose of controlling the relative humidity, the saturated salts solution is inserted into the humidity chamber. In a small closed place, KNO_3 increases the relative humidity up to 95 % at 295 K, while $ZnCl_2$ decreases the relative humidity to 13 %. The relative humidity in the chamber is monitored by a commercial humidity sensor, placed next to the sample. This sensor, obtained from Honeywell (IH-3610-1), has a accuracy of 2 % from 0 to 100 % relative humidity. A voltage of 5 V is feed to the sensor by a Tes power supply.

A silicon photo detector (Thorlabs PDA55) is used to measure the intensity of the light that is guided in the POF and reach the output end of the fiber. This device converts optical signal to electric voltage. This fiber output voltage is read through a multimeter (FLUKE 8840A). To establish the humidity response of the POF, the output voltage is recorded using a labview computer program.

After preparing the experimental setup, the humidity chamber is closed and the computer program is started to record the fiber output voltage and the relative humidity every 3 seconds.

3.4. PEG-Si Coated POF Inside Big Humidity Chamber

PEG-Si coated plastic optical fiber sensor head is placed into the big humidity chamber that has a volume of 12×8×8 cm^3. In this humidity chamber, the relative humidity has a range from 18 % to 80 %. At first, the relative humidity is decreased from 40 % to 18 % by using $ZnCl_2$ saturated salt solution. Figure 3.5 shows the hysteresis response of the POF sensor. The sensor responds quickly to the changes in relative humidity.

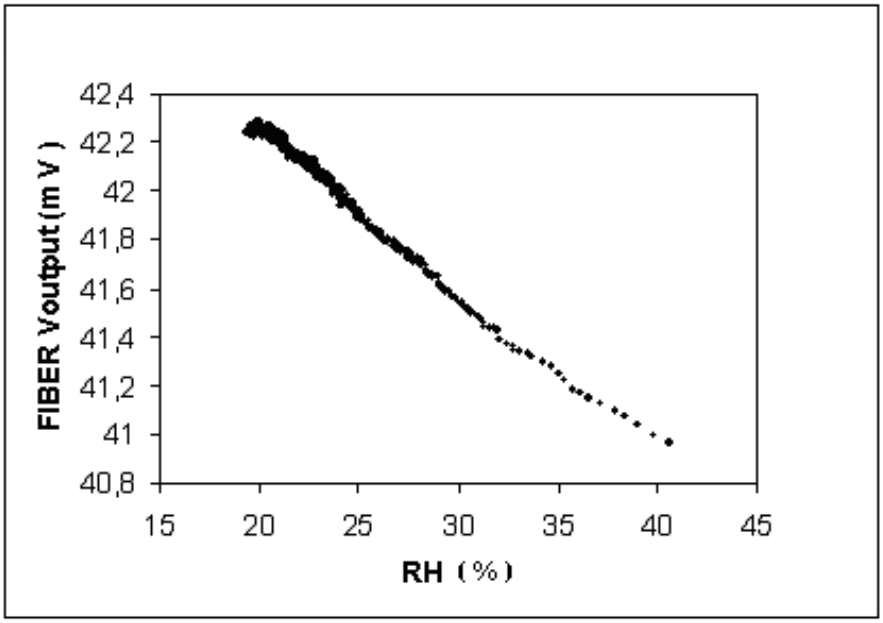

Figure 3.5. The response of the POF sensor at low humidity values

Polymers, in general, are sensitive to water vapor. PEG is one of these highly hydrophilic polymers and is a very good candidate for humidity sensing applications. However, it is easily soluble at high humidity values and comes off the PMMA substrate. Therefore, PEG is cross-linked by synthesizing it together with triethoxy silane, which crosslinks by removal of the ethanol in the presence of acid or base catalyst and reacts chemically with the functional groups present on the PMMA surface, hence providing a crosslinked structure between the PEG molecules themselves as well as the POF surface [21]. The outcome PEG-Si overlay is non-soluble in high water vapors, robust and durable at plastic optical fibre surface. When it is exposed to water vapor, as it absorbs the water molecules, its refractive index changes. At low humidity values the PEG-Si polymer has a semicrystalline form and this semicrystalline form becomes more regular by the attachment of water molecules. Thus, when the amount of the absorbed water molecules by the PEG-Si film increases, its refractive index decreases [22], the sensor head operates as a leaky-type POF. A fraction of the optical power in the fiber core is lost into the overlay in this type fibers when the light launched in the fiber reaches the coated portion of the fiber. Therefore, the light intensity passing through the sensor head changes remarkably depending on the relative humidity. For low values of RH, as the relative humidity increases, the fiber output voltage decreases (see Figure 3.5).

To establish the full responsivity curve of the POF type sensor, KNO_3 saturated salt solution is inserted into the humidity chamber. This solution increases the relative humidity from 40 % to 80 %. Inside this big humidity chamber, the increase rate of the humidity is 0,19 $\%RH/min$ between 40 % and 55 %, above that humidity level the rate drops to 0,0005 $\%RH/min$. As can be clearly seen in Figure 3.7, the sensor output versus humidity curve first of all shows a linear decrease between 18% and 62 % RH with a slope 0,06 $mV/\%RH$, due to operating as a leaky type POF ; then the sensor's response demonstrates a turning point at around 62 % RH. A relatively steeper increase in the detected signal is recorded beyond 62 % RH value with slope 0,083 $mV/\%RH$. The increase in the relative humidity increases the content of the water inside the polymer network, and the polymer starts to swell. At that point, the film changes phase from semicrystalline to a gel form and its refractive index decreases

even further. After swelling, the refractive index in the cladding layer becomes much lower than that of core. The POF structure changes to the guided type and the light intensity passing through the sensor head increases remarkably (see Figure 3.6) [18,19]. As a result of this, a turning point is observed at the fiber output voltage. The net result can be predicted as there is a phase change in the PEG from semi-crystalline to gel form.

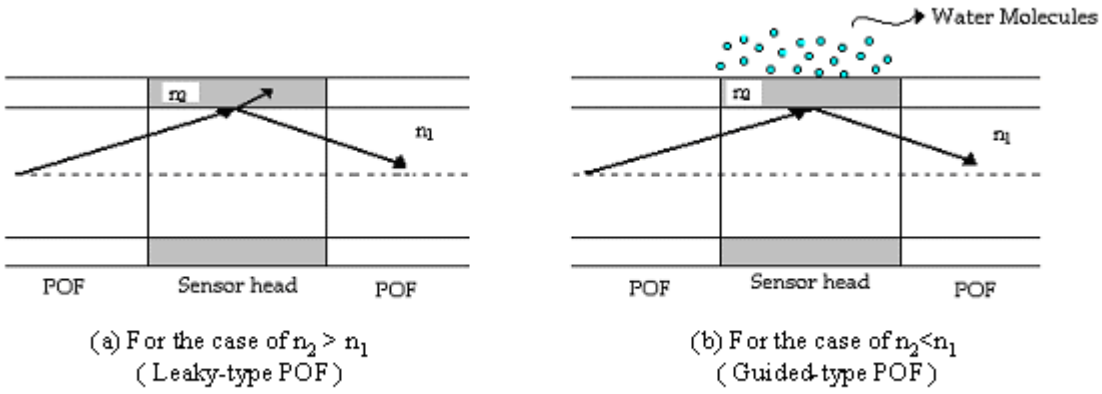

Figure 3.6. The simulation model of the POF humidity sensor

The changes in the index of refraction of the cladding layer of the POF sensor head cause the intensity of the light that is transmitted in the fiber optic to change. The relation between the intensity of the light launched in the fiber and the cladding refractive index can be clarified with the definition of the transmission coefficient of the fiber optics. It is determined by the following four factors (a) NA numerical aperture, (b)PF packing fraction of core area to total area, (c) Fresnel reflectional losses (T_f), (d) internal transmittance of the core (T_i). The transmission can be expressed as follows:

$$T = (NA)^2 \times PF \times T_f \times T_i \tag{3.1}$$

$$NA = \sqrt{(n_{core}^2 - n_{cladding}^2)} \tag{3.2}$$

$$T_i = e^{-\mu l} \tag{3.3}$$

where l is the length of the component, μ is the absorption coefficient of the core. Thus, the power of the light intensity launched in the fiber will depend upon various factors including the square of the numerical aperture [11]. It is obvious that the refractive index of the cladding layer, $n_{cladding}$, affects the numerical aperture and transmission coefficient T. This theoretical model supports our experimental results.

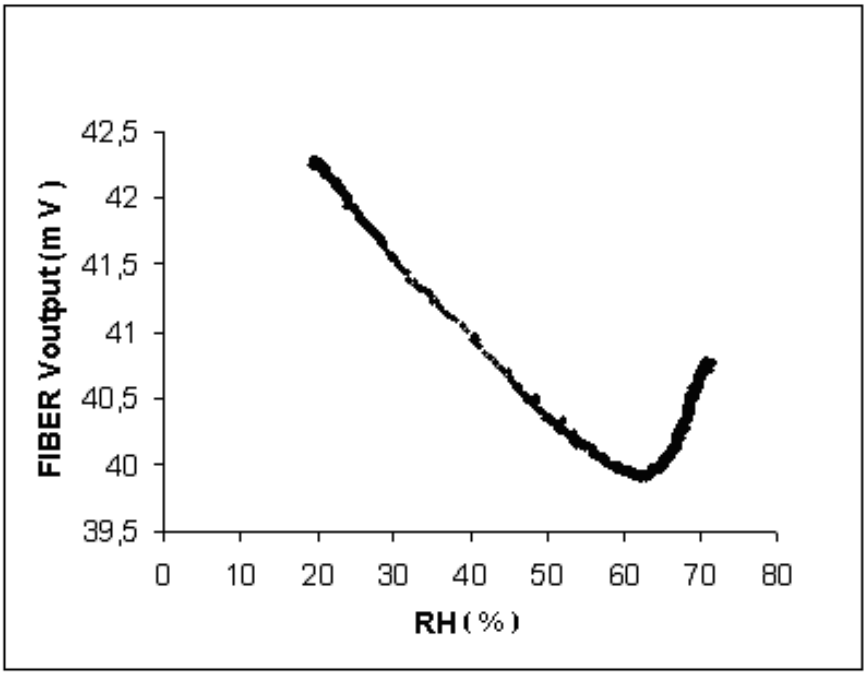

Figure 3.7. Variation of output power in a different humidity environment

3.5. PEG-Si Coated POF Inside Small Humidity Chamber

A good humidity sensor is expected to operate in a wide humidity range. In the big humidity chamber, the humidity range is 18 % to 80 %. In order to expand the humidity range of the sensor, the humidity chamber is exchanged with a smaller one. Using a different chamber also effects the humidity increase rate. Therefore, the relation between the increase rate of the relative humidity and fiber output voltage can be probed. The same experimental setup is constructed using this small humidity chamber. When $ZnCl_2$ saturated salt solution is inserted into the small humidity chamber, the relative humidity decreases from 40 % to 12 %. Figure 3.8 shows the variation of the fiber output voltage with change in the relative humidity for Sample 2, which is coated three times. The variation is approximately linear. It may be noted

that as the humidity decreases the output voltage increases up to 15 %. The gradient of the increasing humidity curve from 40% RH to 15 % RH is 0.12 V/%RH. After this humidity level, the fiber output voltage changes its characteristics and starts to decrease. In other words, there is a turning point at about 15 % humidity level.

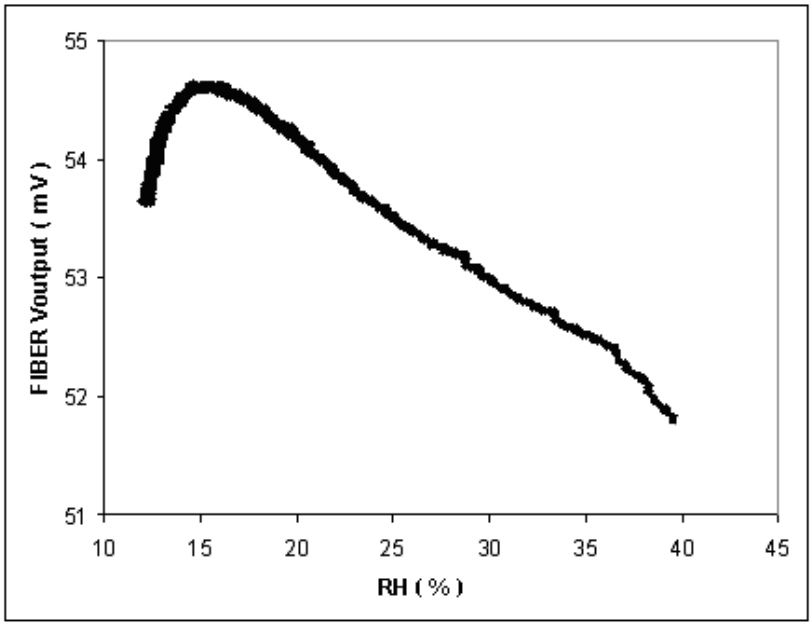

Figure 3.8. The humidity sensor response at low RH levels

KNO_3 saturated salt solution is used to determine the response of the POF type sensor at high humidity values. The measurements that are carried out for an increasing humidity cycle are depicted in Figure 3.9. Inside this small humidity chamber, the ramp rate of the relative humidity is 2 $\%RH/min$. Due to the small volume of the chamber, humidity increases rapidly. It may be noted that as humidity in the chamber increases, the fiber output voltage decreases up to 82 % RH. The gradient of the increasing humidity curve from 18 % to 82 % is 0.12 $V/\%RH$. After the relative humidity inside the chamber is 82 %, the fiber output voltage starts to increase and a turning point is formed. The fiber output voltage continues to increase up to 89 % RH with a gradient 0.21 $V/\%RH$; then it becomes stable.

The rapid increase in the relative humidity inside the chamber causes the responsivity of the humidity sensor to change remarkably. First of all, the humidity level in which PEG-Si starts to swell is 82 % for the high humidity increase rate (2 $\%RH/min.$),

whereas it is 62 % for lower humidity increase rate (0,19 $\%RH/min.$). The swelling ratio of a polymer layer is affected from the humidity ramp rate [40]. During water absorption, the critical humidity where the thin film starts to show a rapid swelling and changes phase from semicrystalline form to gel form shifts to higher humidity, so the turning point in the fiber output voltage versus relative humidity curve also shifts to a somewhat higher value. The second change in the hysteresis is that the sensitivity of the POF humidity sensor increases as the ramp rate of the humidity increases. In addition to high sensitivity, another turning point is observed at very low humidity values such as 15 % RH.

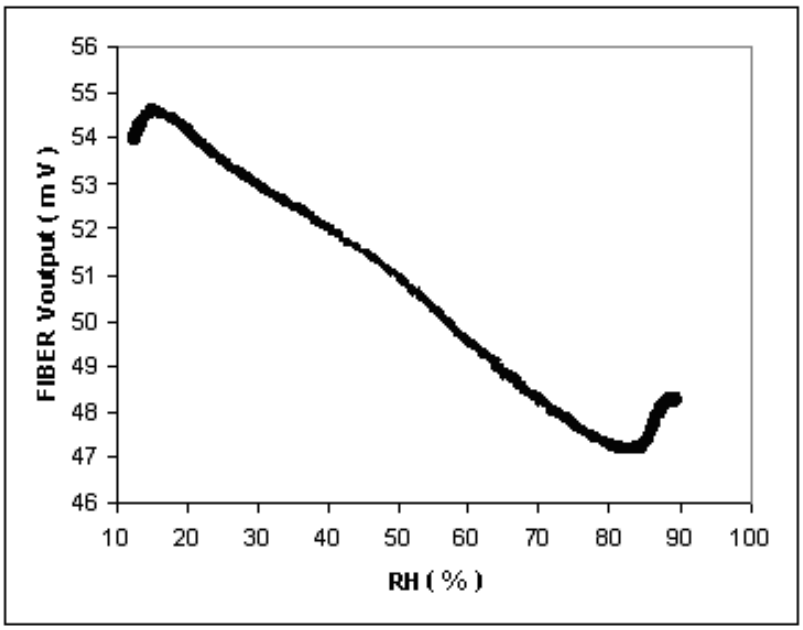

Figure 3.9. The humidity sensor response between 12 % RH and 92 % RH

3.6. Effect of The Membrane Thickness on The Swelling Behavior of The PEG-Si Film

An experimental investigation is conducted to determine the effect of the membrane thickness on the POF type humidity sensor. For this purpose, two samples which have different thickness are used. To prepare a thick sample, polymer solution is flowed through the sample three times over with a constant speed of 10 $ml/min.$ Figure 3.10 shows the effect of different thicknesses on the response of the POF sensor. It can be observed from Figure 3.10 that the thin film coated POF type sensor shows a better

response than the thicker film. For the thin film coated sensor, the decrease rate of the fiber output voltage is 0.11 $V/\%RH$, while it is 0.023 $V/\%RH$ for the thick one. As a result of this, it may be noted that the film thickness is an important property in constructing sensors with higher sensitivity.

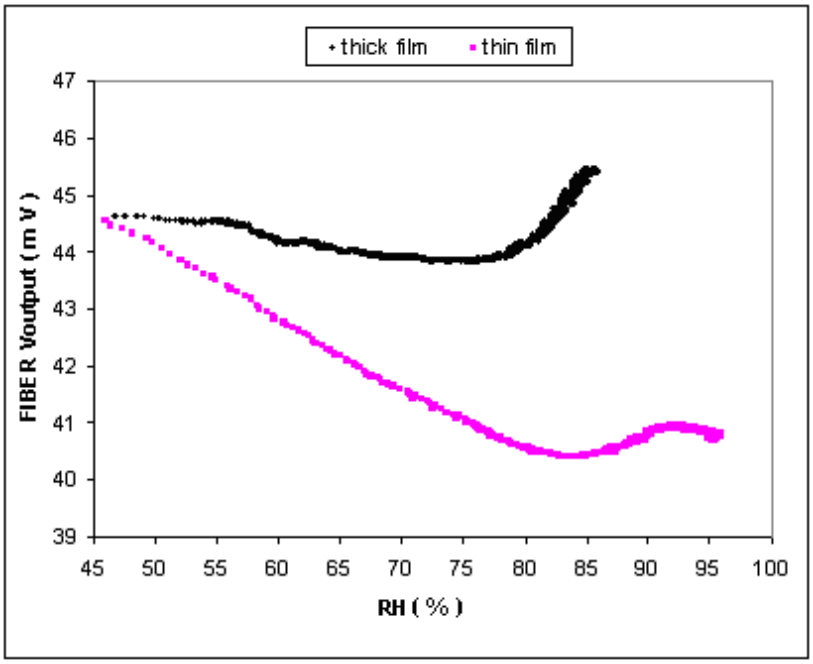

Figure 3.10. The sensor response for different membrane thickness

The second important observation is that increasing the thickness of the membrane causes the turning point to shift to slightly lower humidity values. Water molecules can penetrate into thicker polymer networks easily. Therefore, a thicker film shows a rapid swelling at lower humidity values. After the PEG-Si film swells and a gel form occurs, the fiber output voltage starts to increase with a rate 0.18 $V/\%RH$. As the relative humidity increases in the environment, the steeper increase in the fiber output voltage continues because building up the water molecules inside the PEG-Si network takes more time. Besides, releasing these water molecules is more difficult and sometimes becomes impossible to take out from the polymer network.Therefore, the thin PEG-Si network is more suitable as a sensing film.

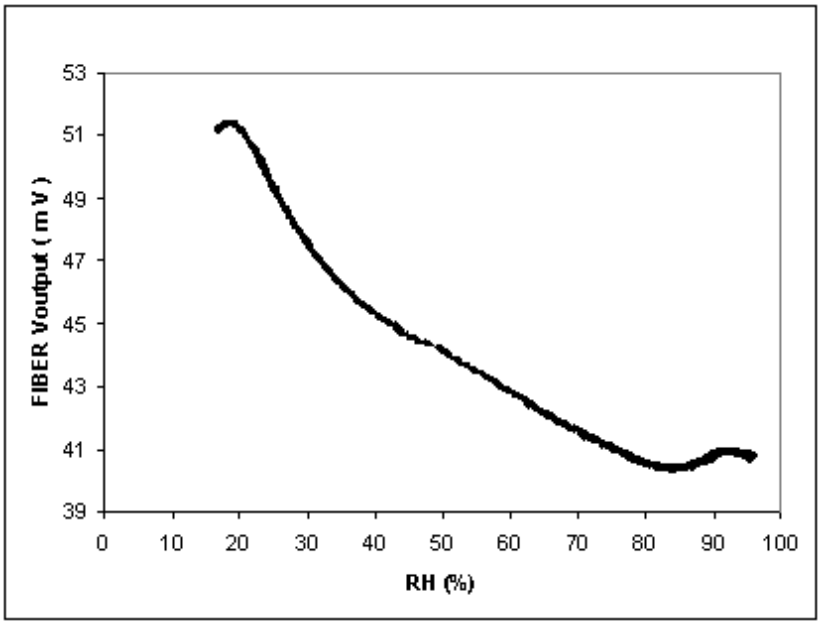

Figure 3.11. The responsivity curve of a thin film coated sensor (Sample1)

3.7. Humidity Responsivity of a Thin PEG-Si Film

During the experimental work, it was realized that the POF type sensor head should be fabricated by coating a very thin PEG-Si network in order to construct a highly sensitive and real humidity sensor. Sample 1 is used as a thin film coated sensor and the full responsivity curve of this sample is given in Figure 3.11. As can be seen from Figure 3.11, the responsivity curve shows different slopes, giving three different humidity regions.The slope of the curve is 0.36 $V/\%RH$ between 20 % and 35 %, 0.12 between 35 % and 82 %, 0.125 after 82 %. The sensor exhibits higher sensitivity at low humidity levels. The sensor response is not linear because of the interaction of the water molecules with PEG's brushes. It demonstrates three turning points at around 20 %, 82 % and 92 %. The cause of these turning points is that polyethylene glycol changes phase from semicrystalline form to gel form and its refractive index changes with respect to the content of water molecules. The refractive index of the PEG-Si decreases as humidity increases up to 82 %. Because the diffusion of the water vapor molecules into the PEG-Si polymer network slightly reduces the optical density of the polymer film, turning into a less semi-crystalline structure; thus $n_{cladding}$ decreases. As the water molecules start to saturate between the PEG-Si brushes, that is, above

82 %, a significant swelling occurs in the PEG-Si film; thus reducing the density and hence n_{PEG-Si} significantly [22]. As a result of this instability of the PEG-Si, turning points are observed at 20 % and 82 % humidity values. To deal with this instability problem observed in the PEG-Si network at high humidity values and also to increase the range of RH in which measurements can be done with PEG-Si, the PEG-Si samples are enriched with hydrogen.

3.8. Humidity Responsivity of a Hydrogenated Thin PEG-Si Film

When PEG-Si is exposed to water vapor, hydrogen atoms of the water molecules make bonds with the ether oxygen atoms in the PEG chain. Because of the influence of the absorbed water molecules, PEG-Si network swells and changes its phase from semi-crystalline to gel form. To construct a stable sensor, this swelling should be prevented or at least delayed. The easiest way of obtaining a stable PEG-Si network is to decrease the amount of ether oxygens that can bind with water molecules. Hydrogen gas is used to reduce the number of ether oxygen sites. When a PEG-Si network is exposed to hydrogen gases, hydrogen molecules make bonds with the ether oxygen atoms, and their number decreases. Consequently, it is expected that the turning point occurring at the high humidity value disappears and the sensor humidity response becomes perfectly linear at the expense of a reduced sensitivity.

In order to hydrogenate PEG-Si coated samples, they are first heated in a vacuum chamber for two hours at a pressure of 10^{-4} Pa. After annealing the samples, the chamber is filled with hydrogen gas to a pressure of 10 Pa, and they are kept in it for another 80 minutes.Then, the hydrogenated sample is inserted into the humidity chamber. In order to study the response characteristics of the hydrogenated sensor, measurements are carried out for different relative humidity values in the chamber. Figure 3.12 shows the variation of fiber output voltage with change in relative humidity for a hydrogenated thick film, (Sample 2). Measurements on hydrogenated Sample 2 show that the general characteristics of the sensor are nearly the same as in the previous measurements. However, the turning point that occurs at low humidity values slightly shifts to a somewhat lower humidity value, while the turning point at 82 % shifts to

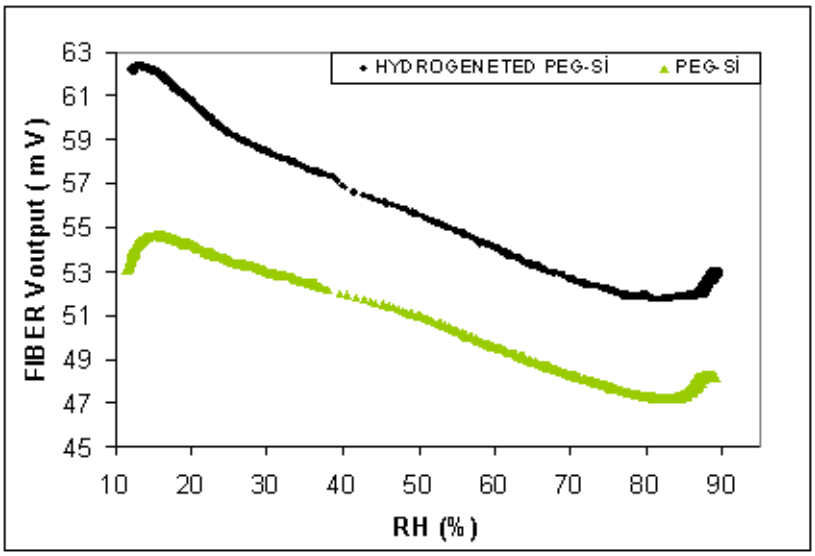

Figure 3.12. The relative humidity response of Sample 2 (thick sample) before and after hydrogenation

a slightly higher humidity value. Because of the film thickness, the sensor response versus humidity has not become perfectly linear and the turning points could not be permanently straightened.

The hydrogenation process is repeated for Sample 1 (thin sample), and the humidity response of the thin film coated POF sensor is shown in Figure 3.13. It should be noted that the sensor response becomes almost linear between 14 % and 89 % relative humidity values. After hydrogenating the PEG-Si film, it becomes less hydrophilic and absorbs less water molecules. Therefore, PEG-Si starts to swell at higher humidity value. In this POF type sensor, swelling starts at 89 % RH value after the sample is enhanced with hydrogen.

Next, the experimental calibration curve for humidity is also taken. The experimental result is shown in Figure 3.14, in which a fine pink curve shows the data measured using a calibrated electronic real humidity sensor, and a thick black curve shows the hydrogenated fiber output voltage change of the POF-type sensor. From this figure, the optical humidity sensor presented is confirmed to operate over a wide humidity range from 45 % to 80 %. Judging from these excellent properties, this

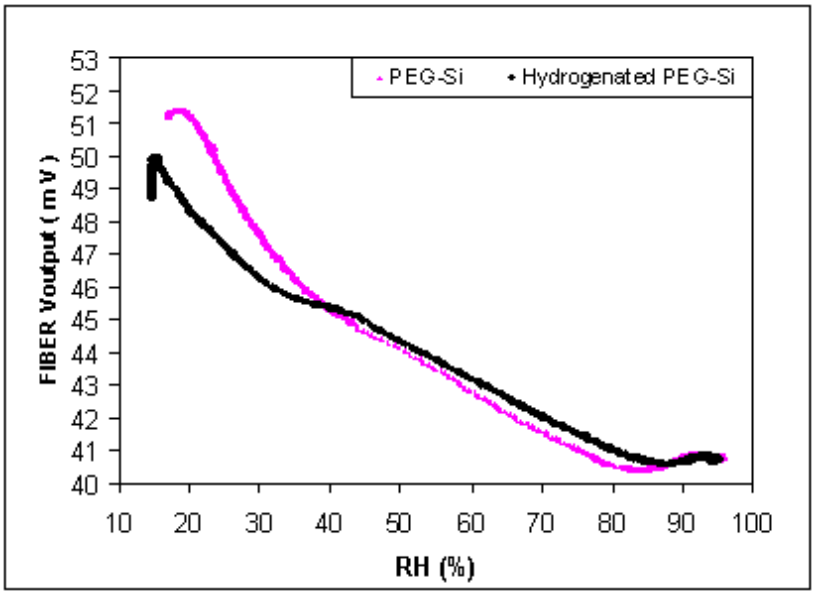

Figure 3.13. The relative humidity response of Sample 1 (thin sample) before and after hydrogenation

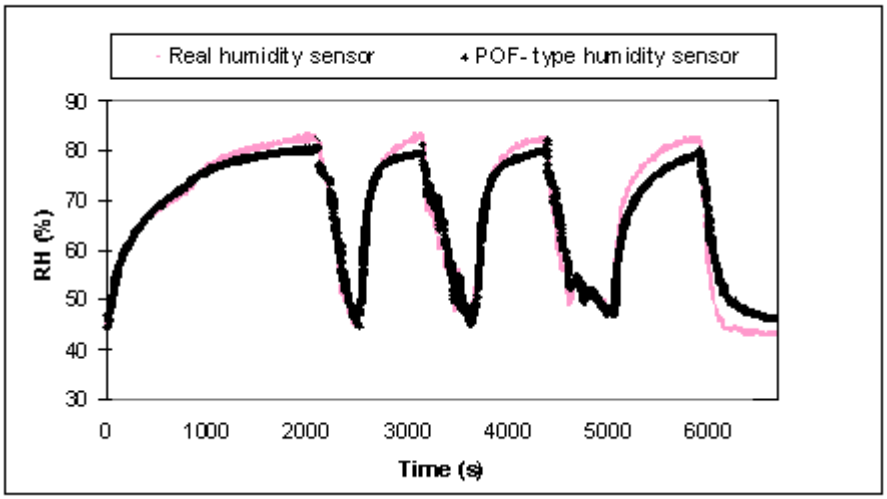

Figure 3.14. Hydrogenated POF-type sensor and a real sensor outputs

POF-type sensor could be used for real-time humidity monitoring.

3.9. Effects of The Various Gases on PEG-Si Thin Film

In many fields, such as environmental pollution, biotechnology, chemical analysis and on-line control of production lines, control of gasses becomes very important.

There are several environmental gas sensors, e.g. liquid and solid state electrochemical sensors for ionic and neutral gas concentrations, semiconducting oxides, field effect transistor, diode, and SAW type sensors. However, new methods should be investigated to minimize the cost and environmental hazard of the gas sensors. In view of this, we have studied a new optical gas sensor using plastic optical fibres. This POF type sensor head can be easily prepared by coating PEG-Si polymer layer on the plastic fibre core. When exposed to chemical vapor, the light intensity passing through the fiber remarkably changes because of the gas molecules diffusing into the PEG-Si polymer layer.

In this thesis, the response of the PEG-Si coated fiber to various gasses such as methanol, acetone, hexane, benzene, and toluene is studied. Some special properties of these gasses are given in Figure 3.15.

For gas sensor measurements, the same setup is used as shown in Figure 3.4. But, instead of saturated salt solutions, the liquid form of gasses is inserted into the closed chamber. Firstly, 10 ml liquid methanol (CH_3OH) is placed into the chamber at 298 K and the fiber output voltage is recorded. When PEG-Si is exposed to methanol vapor, the polymer can easily absorb the methanol molecules. Generally, alcohol groups penetrate into the polymer layer by means of O-H bonds. After solvent penetration, the crystallinity of the polymer decreases because of the swelling and commensurate with the formation of gel. Therefore, the effective refractive index of the overlay material decreases and the sensor head starts to operate as a guided-type POF. As a result, the fiber output voltage shows a steeper increase as shown in Figure 3.16. Then the increase rate of the output voltage slows down and becomes nearly stable after 200 min.

From Figure 3.16 and 3.17, it can be concluded that the response of the polymer film to both acetone and methanol vapor are showing the same characteristics except that the increase in the output voltage values upon the absorption of acetone vapor is nearly 10 mV greater than the increase upon the absorption of the methanol vapor. Acetone is a better solvent than methanol. Depending on that, acetone molecules can

	Molecular Formula	Molecular Structure	Refractive Index	Group
METHANOL	CH_3OH	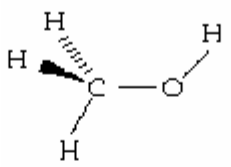	1,3284	Alcohol
ACETONE	CH_3COCH_3	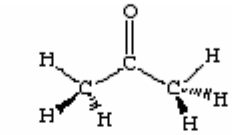	1,3590	Ketone
BENZENE	C_6H_6	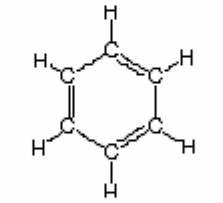	1,5011	Aromatic
TOLUENE	C_7H_8	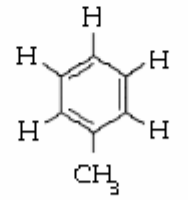	1,4960	Aromatic
HEXANE	C_6H_{14}	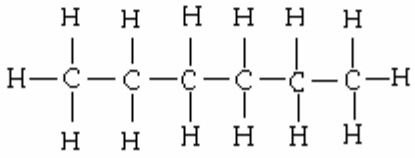	1,3806	Alkane

Figure 3.15. Some properties of the used gases during the experiment

rapidly diffuse into the polymer network, the increase of the output voltage takes less time, and it shows a higher increment than methanol.

On the other hand the response of the PEG-Si to hexane, which belongs to the alkane hydrocarbon group, is also studied during our experiments. Hexane isomers are largely unreactive, and are frequently used as an inert solvent in organic reactions because they are very non-polar. Because of the fact that polymers are polar, gas

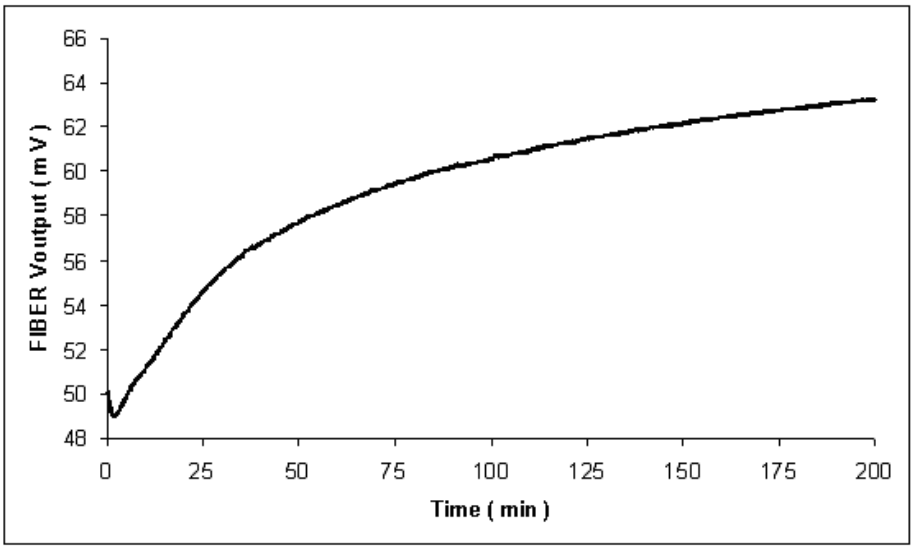

Figure 3.16. The response of POF sensor which is coated PEG-Si to methanol

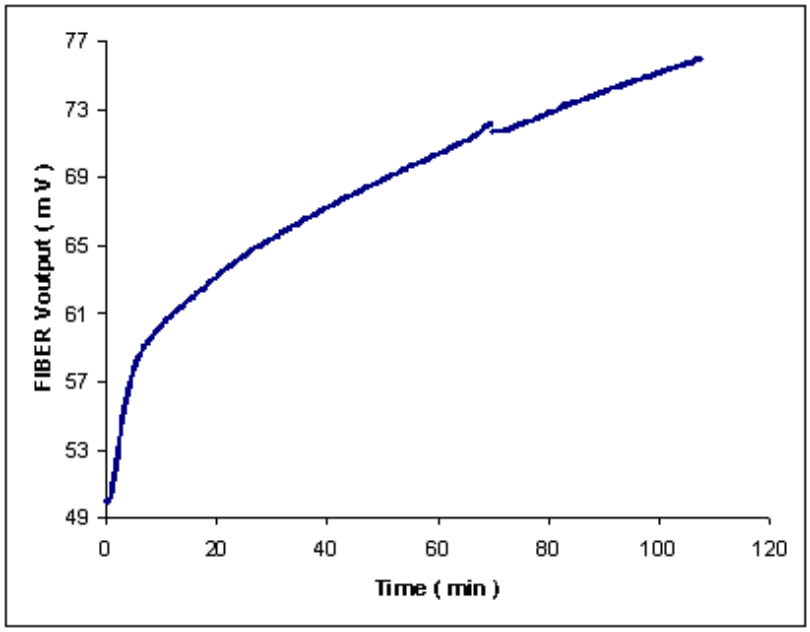

Figure 3.17. The response of POF sensor which is coated PEG-Si to acetone

molecules such as polar alcohols sorb into polar film more than nonpolar ones such as alkanes [46]. In Figure 3.18, it is obvious that the fiber output voltage rapidly increases as by 5 mV; then, it becomes stable after nearly ten minutes.

Finally, aromatic hydrocarbons, toluene and benzene are used to determine the effects of these gases on the fiber output voltage. Benzene and toluene are cyclic

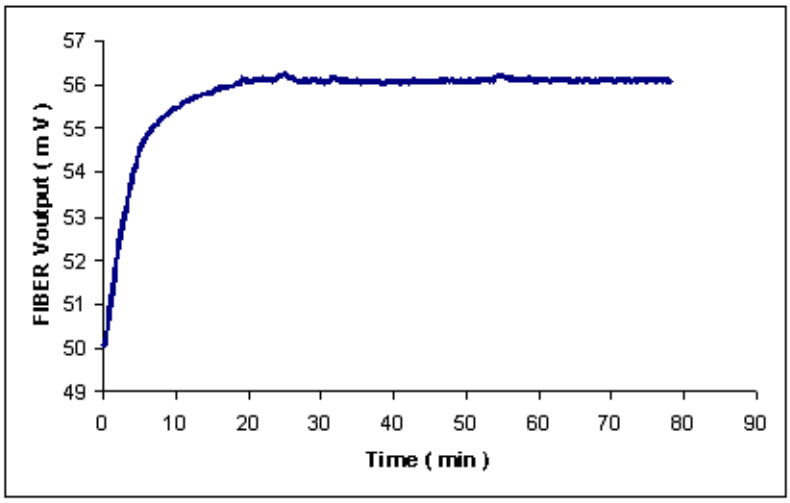

Figure 3.18. The response of POF sensor which is coated PEG-Si to hexane

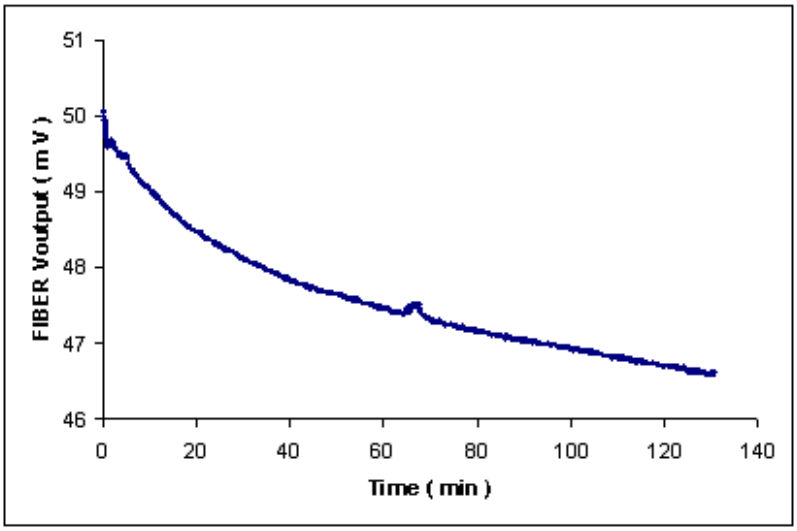

Figure 3.19. The response of POF sensor which is coated PEG-Si to toluene

hydrocarbons with a continuous alternation of single and double bonds. These gases can not easily diffuse into the polymer layer due to their ring structures. The refractive indices of benzene and toluene are 1.5011 and 1.4960, respectively. Therefore, the effective refractive index of the PEG-Si increases when aromatic hydrocarbons diffuse into it. The refractive index of the cladding layer becomes bigger than that of the core and our sensor structure operates as a leaky-type POF. A fraction of the optical power in the fiber core is lost into the overlay; hence, the fiber output voltage starts to decrease (see Figure 3.19 and Figure 3.20).

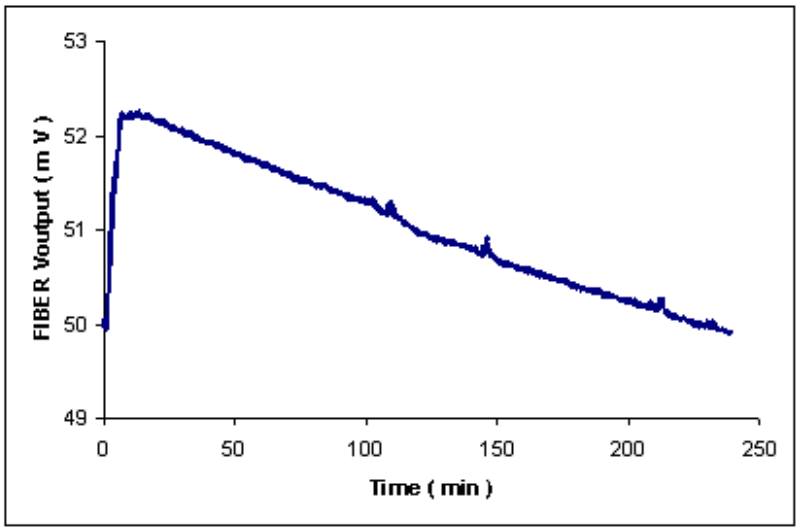

Figure 3.20. The response of POF sensor which is coated PEG-Si to benzene

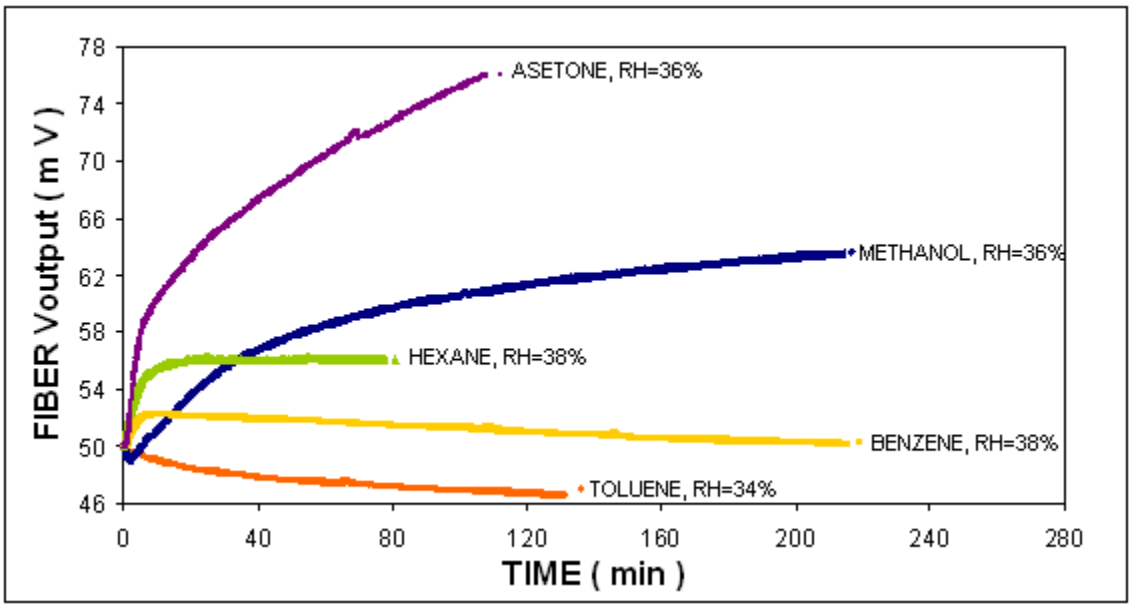

Figure 3.21. POF-type gas sensor responses

4. CONCLUSIONS

In the first part of this work, the changes in the output voltage of a fiber, which is coated with pure and hydrogenated PEG-Si thin films, are studied under changing relative humidity from 13 % to 95 % . It is observed that PEG-Si is highly sensitive to the changes in relative humidity. When the PEG-Si is dry, its refractive index ($n_{cladding}$) is slightly smaller than the refractive index of fiber core (n_{core}); it then operates as a leaky-type POF. For this type of the plastic optical fibers, coupling occurs, and a fraction of the power in the fiber core is lost into the overlay. This fraction depends on the amount of polishing done during manufacture; it increases as the polishing approaches the core. As the relative humidity increases, ($n_{cladding}$) decreases more because of the fact that the diffusion of water vapor molecules into the PEG-Si polymer network reduces the optical density of the overlay film, turning it into a less semi-crystalline structure. Hence, the fiber output voltage decreases further with increasing relative humidity up to 80 %. After 80 % RH value, the polymer melts from the semicrystalline form to gel form and its refractive index shows a sudden and steeper decrease [22]. After this situation the optical power leakage into overlay goes down as a result of lowering of the optical density. Beyond 80 %, the sensor head operates as a guided-type POF. This is why a turning point occurs in the PEG-Si sensor response at around 80 % RH and consequently the fiber output voltage gradually shows a steeper increase as the relative humidity raises from 80 % to 90 %. The swelling process of a polymer layer is an instability problem and affects the reliability and performance of the sensor adversely. Moreover the sensor is not repeatable; the polymer film should be dried after each measurement to make successive measurements. After drying, the polymer film could reach its pre-absorption form by giving off all the water molecules absorbed.

It is also observed that the rate of humidity change and the thickness of the polymer film change the response hysteresis of the sensor. If the relative humidity change rate decreases, the polymer film starts to swell at a lower humidity value (62 % RH).

To overcome the instability problem of the PEG-Si polymer film, it is enriched with hydrogen molecules. These hydrogen molecules make bonds with the ether oxygen of the polymer film; hence, the number of ether oxygen atoms that can bind to water molecules decreases. As a result, the hydrogenated PEG-Si film shows a more stable behavior than the pure PEG-Si film and the turning point shifts to 89 % relative humidity value. Thus, our fiber optic humidity sensor gives a fairly repeatable, linear, and fast response for the humidity range from 13 % to 90 %.

In the second part, the response of PEG-Si film to the vapor of acetone, methanol, hexane, toluene, and benzene is studied. It is observed that the fiber output voltage significantly changes when a polymer film coated sensor head is exposed to these gases. PEG-Si gives the highest response to acetone and methanol. Results indicate that the differences in polymer-solvent interactions result in a much larger adsorption of acetone than methanol. Since hexane has a large molecular structure, only a small number of hexane molecules can penetrate into the polymer film; therefore the fiber output voltage shows a little rise. PEG-Si also shows sensitivity to benzene and toluene. The refractive indices of benzene and toluene are 1.5011 and 1.4960, respectively. The refractive indices of these gases are bigger than that of the core. After toluene and benzene molecules diffuse into the polymer, the effective refractive index of the cladding layer becomes bigger than the core refractive index and it operates as a leaky-type POF. Therefore, the fiber output voltage decreases. According to these results, PEG-Si coated POF can be used as a gas sensor.

From all of these experimentally observed properties, it can be concluded that PEG-Si has a potential for use in humidity and gas sensing devices. This kind of polymer based fiber optic humidity sensors can be very useful in medical applications since PEG is not a hazardous material.

REFERENCES

1. Choi, M.M.F., "Humidity-sensitive optode membrane based on a fluorescent dye immobilized in gelatin film", Vol.378, pp. 127-134, 1999.

2. Ballantine, D. S. and H. Wohltjen, "Optical waveguide humidity detector", *Anal. Chem.*, Vol.58, pp. 2883-2885, 1986.

3. Weiss, M. N., R. Srivastava and H. Groger, "Experimental investigation of a surface plasmon-based integrated-optic humidity sensor", *Electronics Letters*, Vol.32, pp. 842-843, 1996.

4. Feng, C. -D., S. -L. Sun, H. Wang, C. U. Segre and J. R. Stetter, "Humidity sensing properties of Nafion and sol-gel derived SiO_2/Nafion composite thin films", *Sensors and Actuators B*, Vol.40, pp.217-222, 1997.

5. Erdamar, O., Y. Skarlatos, G. Aktas and M. N. Inci, "Experimental investigation of the conduction mechanism of hydrogenated PEG thin films at high relative humidities", *Solid State Ionics*, Vol.177, pp. 3217-3221, 2006.

6. Huang, H. and P. K. Dasgupta, "Perfluorosulfonate ionomer-phosphorus pentoxide composite thin films as amperometric sensors for water", *Anal. Chem.*, Vol.53, pp. 1570-1573, 1991.

7. Matsuguch, M., T. Kuroiwa, T. Miyagishi, S. Suzuki, T. Ogura and Y. Sakai, "Stability and reliability of capacitive-type humidity sensors using crosslinked polyimide films", *Sensors and Actuators B*, Vol.52, pp. 53-57, 1998.

8. Boltinghouse, F. and K. Abel, "Development of an optical relative humidity sensor. Cobalt chloride optical absorbency sensor study", *Anal. Chem.*, Vol.61, pp. 1863-1866, 1989.

9. Pincenti, J. C. and D. L. Naylor, "Humidity dependence of the birefringence in poly(methyl methacrylate) waveguides", *Applied Optics*, Vol.33, pp. 1090-1094, 1994.

10. Glenn, S. J., B. M. Cullum, R. B. Nair, D. A. Nivens, C. J. Murphy and S. M. Angel, "Lifetime based fiber optic water sensor using a luminescent complex in a lithium-terated Nafion membrane", *Analytica Chimica Acta*, Vol.448, pp. 1-8, 2001.

11. Shukla, S. K., G. K. Parashar, A. P. Mishra, Puneet Misra, B. C. Yadav, R. K. Shukla, L. M. Bali and G. C. Dubey, "Nano-like magnesium oxide films and its significance in optical fiber humidity sensor", *Sensors and Actuators B*, Vol. 98, pp. 5-11, 2004.

12. Ansari, Z. A., R. N. Karekar and R. C. Aiyer, "Humidity sensor using planar optical waveguides with claddings of various oxide materials", *Thin Solid Films*, Vol. 305, pp. 330-335, 1997.

13. Ballantine, D. S. and H. Wohltjen, "Optical waveguide humidity sensor", *Anal. Chem.*, Vol. 58, pp. 2883-2885, 1986.

14. Tay, C. M., K. M. Tan, S. C. Tjin, C. C. Chan and H. Rahardjo,"Humidity sensing using plastic optical fibers", *Microwave and Optical Technology Letters*, Vol.43, pp. 387-390, 2004.

15. Corera, Fátima Pérez and Ainhoa Gastón, Joaquín Sevilla, "Relative humidity sensor based on side-polished fiber optic", *Instrumentation and Measurement Technology Conference, 2000*, Vol.1, pp. 17-22, 2000.

16. Bownass, D. C., J. S. Barton and J. D. C. Jones, "Serially multiplexed point sensor for the detection of high humidity in passive optical networks", *Optics Letters*,Vol.22, No.5, pp. 346-348, 1997.

17. Morisawa, M. and S. Muto, "A novel breathing condition sensor using plastic optical fiber", *Sensors*, Vol.3, pp. 1277-1280, 2004.

18. Muto, S., O. Suzuki, T. Amano and M. Morisawa, "A plastic optical fibre sensor for real-time humidity monitoring", *Measurement Science and Technology*, Vol.14, pp. 746-750, 2003.

19. Suzuki, O., M. Miura, M. Morisawa and S. Muto, "POF-type optic humidity sensor and its application", *IEEE*, Vol.1, pp. 447-450, 2002.

20. Bownass, D. C., J. S. Barton and J. D. C. Jones, "Detection of high humidity by optical fibre sensing at telecommunications wavelengths", *Optics Communications*, Vol.146, pp. 90-94, 1998.

21. Yogun, H. U., Y. Ercil, Y. Menceloglu and N. Inci, "Coating material and a fiber optic sensor in which this coating material is used", *European Patent*, Publication No.WO2005090253, 2005.

22. Bilen, B., "Effects of gases on optical properties of polyethylene glycol", Phd. Thesis, Bogazici Uni., 2007.

23. Keiser, G., Optical fiber communications, Second Edition, New York, McGraw-Hill Inc, 1991.

24. Wilson, J. and J.F.B. Hawkes, Optoelectronics An Introduction, Second Edition, New York, Prentice Hall, 1989.

25. Kasap, S. O., Optoelectronics And Photonics, First Edition, New York, Prentice Hall, 2001.

26. Inci, M. N., "Optical coatings for fiber optic sensors", Phd., Heriot-Watt University, 1992.

27. Senior, J. M., Optical fiber communications: Principles and practice, New York,

Prentice Hall, 1992.

28. Pollock, C. R., Fundamentals of optoelectronics, Chicago, 1995.

29. Udd, E., Fiber optic smart structures, New York, Wiley-Interscience, 1995.

30. Yeo, T. L., T. Sun, K. T. V. Grattan, D. Parry, R. Lade and B.D. Powell, "Polymer-coated fiber bragg grating for relative humidity sensing", *IEEE Sensors Journal*, Vol.5, pp. 1082-1089, 2005.

31. Dakin, J. and B. Culshaw, Optical Fiber Sensors: Principles and Components, Vol.2, Boston and London, Artec House, 1988.

32. Arregui, F. J., Y. Liu, I. R. Matias and R. O. Claus, "Optical fiber humidity sensor using a nano Fabry-Perot cavity formed by the ionic self-assembly method", *Sensors and Actuators B*, Vol.59, pp. 54-59, 1999.

33. Otsuki, S., K. Adachi and T. Taguchi, "A novel fiber optic gas sensing arrangement based on an air Gap design and an application to optical detection of humidity", *Analytical Sciences*, Vol.14, pp. 633-635, 1998.

34. Matsuguchi, M., Y. Sadaoka, H. Mizuguchi, K. Umeda and Y. Sakai, "Solvatochromic study of water sorption in polymer films", *J. Appl. Polym. Sci.*, Vol.63, pp. 1681-1691, 1997.

35. Ichkawa, K., T. Mori, H. Kitano, M. Fukuda, A. Mochizuki and M. Tanaka, "Fourier transform infrared study on the sorption of water to various kinds of polymer thin films", *J. of Polym. Sci. Part B*, Vol.39, pp. 2175-2182, 2001.

36. Adhikari, B. and S. Majumdar, "Polymers in sensor applications", *Prog. Polym. Sci.*, Vol.29, pp. 699-766, 2004.

37. Matsuguchi, M., S. Umeda, Y. Sadaoka and Y. Sakai, "Characterization of polymers for a capacitive-type humidity sensor based on water sorption behavior",

Sens. Actuators B, Vol.49, pp. 179-185, 1998.

38. Chen, W. and K. R. Shull, "Equilibrium swelling of hydrophilic polyacrylates in humid environments", *Macromolecules*, Vol.32, pp.136-144, 1999.

39. Yang, Z., J. A. Galloway and H. Yu, "Protein interactions with poly(ethylene glycol) self-assembled monolayers on glass substrates: Diffusion and adsorption", *Langmuir*, Vol.15, pp. 8405-8411, 1999.

40. Tae, G., J. A. Kornfield, J. A. Hubbell and D. Johannsmann, "Anomalous sorption in thin films of fluoroalkyl-ended poly(ethylene glycol)s", *Langmuir*, Vol.18, pp. 8241-8245, 2002.

41. Van der Wel, G. K. and O. C. G. Adan, "Moisture in organic coatings-a review", *Progress in Organic Coatings*, Vol.37, pp. 1-14, 1999.

42. Biesalski, M. and J. Rhe, "Swelling of a polyelectrolyte brush in humid air", *Langmuir*, Vol.16, pp. 1943-1950, 2000.

43. Kitano, H., K. Ichikawa, M. Ide, M. Fukuda and W. Mizuno, "Fourier transform infrared study on the state of water sorbed to poly(ethylene glycol) films", *Langmuir*, Vol.17, pp. 1889-1895, 2001.

44. Yogun, H. U., Y. Ercil, Y. Menceloglu and N. Inci, "Coating material and a fiber optic sensor in which this coating material is used", *European Patent*, Publication No.WO2006011117, 2006.

45. Erdamar, O., Y. Skarlatos, G. Aktas and M.N. Inci, "Experimental investigation of the humidity induced change in the conduction mechanism of PEG", *Appl. Phys. A*, Vol.83, pp. 159-162, 2005.

46. Nakamura, K., T. Nakamoto and T. Moriizumi, "Prediction of QCM gas sensor responses and calculation of electrostatic contribution to sensor responses using a computational chemistry method", *Materials Science and Engineering C*, Vol.12,

pp. 3-7, 2000.